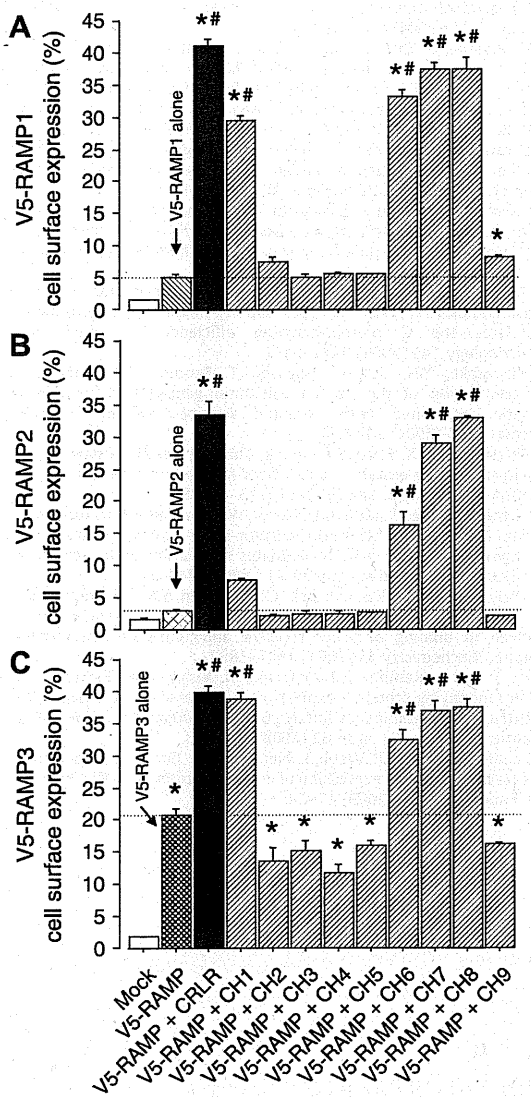

Fig. 4. FACS analysis of the cell surface expression of V5-RAMP1 (A), V5-RAMP2 (B), and V5-RAMP3 (C) following transfection into HEK-293 cells, with or without CRLR or CRLR/VPAC2 chimeras. After transfection, cells were analyzed as in Fig. 1. Bars represent means ± SEM of three experiments. $^{*}p < 0.03$ vs. Mock; $^{\#}p < 0.005$ vs. the corresponding V5-RAMP alone.

tion with RAMP in HEK-293 cells [16] or COS-7 cells [17], reflecting the efficient self-transport of the CT receptor to the cell surface. Our present findings show that the self-transport of VPAC2 is very similar to that of the CT receptor. Notably, overexpression of the CT receptor leads to marked increases in the surface delivery of V5-RAMPs [12,18], but overexpression of VPAC2 did not. Thus translocation of GPCRs to the cell surface may not be a useful marker of RAMP–GPCR interaction. On the other hand, surface delivery of V5-RAMP1, -2 and -3 in HEK-293 cells was markedly increased by co-transfection of CRLR. These increases were more dramatic than those seen when V5-CRLR was co-transfected with each of the three RAMPs. Thus using FACS to measure the surface delivery of tagged RAMPs co-expressed with GPCRs appears to be an effective means of evaluating trafficking interactions between RAMPs and GPCRs.

In the present study, co-transfection of four chimeras, CH2, -3, -4 and -5, did not lead to increases in cell-surface expression of V5-RAMP1, -2 or -3. Nonetheless, total expression of these chimeras did not significantly differ from that of CRLR in the absence of exogenous RAMPs (Fig. 2B), which suggests that the absence of the surface delivery of V5-RAMPs was not due to diminished synthesis of these chimeras or to their enhanced degradation (e.g., due to misfolding). Collectively then, these results indicate that regions extending from TM1 through TM5 within CRLR are necessary and sufficient for the transport of RAMPs to the plasma membrane. Additional FACS analysis will be needed to determine in detail the specific regions of CRLR involved in their trafficking interactions with RAMPs.

The CRLR/VPAC2 chimera CH9, in which the N-terminus of VPAC2 was replaced with that of CRLR, also failed to increase cell-surface translocation of the three V5-RAMPs in HEK-293 cells. This is consistent with the results obtained with CH2, -3, -4 and -5, probably reflects the presence of VPAC2 sequences in regions extending from TM1 through TM5 in the CH9. Like VPAC2, the secretin and PTH receptors, both of which are Family B GPCRs, do not associate with RAMP1 [4,19]. In contrast to our results, an earlier immunoblot analysis showed that two chimeras in which the N-termini of the secretin and PTH receptors were replaced with that of CRLR, appeared at the cell surface along with RAMP1 in both HEK-293 (tsA 201) [19] and COS-7 [20] cells. On the other hand, neither chimera was capable of signaling with CGRP, despite the fact that both CGRP and a non-peptide CGRP antagonist interact directly with the N-terminus of CRLR in complex with RAMP1 [20,21]. The inconsistency of the data likely reflects differences in chimeric GPCR partners, cell types, and assays of RAMP translocation to the cell surface.

We fond that chimeras CH1, -6, -7 and -8, which possess no VPAC2 sequences in regions extending from TM1 to TM5, increased the surface expression of V5-RAMP1 and -3 to the same degree as CRLR did. Interestingly, CH7 and CH8, but not CH1 or CH6, also increased surface delivery of V5-RAMP2, indicating that the N-terminus, 3rd intracellular loop and/or TM6 within CRLR are also important for selective trafficking interactions with RAMP2. Human RAMP2 is 26 amino acids longer than either hRAMP1 or hRAMP3, and hRAMP1 and -3, but not hRAMP2, possess 11 conserved amino acids in their N-terminus and TM domains [1,2]. The unique features of RAMP2 likely account for its specific trafficking interactions with CRLR.

In summary, we have shown that using flow cytometry to measure cell-surface translocation of the three RAMPs is an effective means of evaluating RAMP–receptor interactions, irrespective of whether GPCRs are capable of self-transport (e.g., CRLR vs. CT receptor). The present FACS analysis also revealed the crucial CRLR regions (from TM1 to TM5) responsible for cell-surface translocation of RAMPs, as well as the differences in trafficking interactions among RAMPs with respect to the N-terminus, 3rd intracellular loop and/or TM6 of CRLR.

Notably, recent work suggests there may be a relationship between RAMP1 and the dopamine receptor, a Family A GPCR [22]. To date, at least seven types of accessory protein, including RAMPs, have been shown to be required for correct targeting of GPCRs to the cell surface [23]. The present FACS analysis should therefore contribute greatly to the identification of additional RAMP-interacting GPCRs, and may also stimulate investigation of other interactions between accessory proteins and their receptor partners.

Acknowledgments

This work was supported in part by a Grant-in-Aid for Scientific Research from the Ministry of Education, Culture, Sports and Science.

References

[1] L.M. McLatchie, N.J. Fraser, M.J. Main, A. Wise, J. Brown, N. Thompson, R. Solari, M.G. Lee, S.M. Foord, RAMPs regulate the transport and ligand specificity of the calcitonin-receptor-like receptor, Nature 393 (1998) 333–339.

[2] D.L. Hay, D.R. Poyner, P.M. Sexton, GPCR modulation by RAMPs, Pharmacol. Ther. 109 (2006) 173–197.
[3] T. Bouschet, S. Martin, J.M. Henley, Regulation of calcium-sensing-receptor trafficking and cell-surface expression by GPCRs and RAMPs, Trends Pharmacol. Sci. 29 (2008) 633–639.
[4] P.M. Sexton, D.R. Sexton, J. Simms, A. Christopoulos, D.L. Hay, Modulating receptor function through RAMPs: can they represent drug targets in themselves?, Drug Discov Today 14 (2009) 413–419.
[5] C. Gibbons, R. Dackor, W. Dunworth, K. Fritz-Six, K.M. Caron, Receptor activity-modifying proteins: RAMPing up adrenomedullin signaling, Mol. Endocrinol. 21 (2007) 783–796.
[6] K. Kuwasako, K. Kitamura, S. Nagata, J. Kato, Functions of the extracellular histidine residues of receptor activity-modifying proteins vary within adrenomedullin receptors, Biochem. Biophys. Res. Commun. 377 (2008) 109–113.
[7] K. Kuwasako, K. Kitamura, Y. Nagoshi, Y.N. Cao, T. Eto, Identification of the human receptor activity-modifying protein 1 domains responsible for agonist binding specificity, J. Biol. Chem. 278 (2003) 22623–22630.
[8] K. Kuwasako, Y. Shimekake, M. Masuda, K. Nakahara, T. Yoshida, M. Kitaura, K. Kitamura, T. Eto, T. Sakata, Visualization of the calcitonin receptor-like receptor and its receptor activity-modifying proteins during internalization and recycling, J. Biol. Chem. 275 (2000) 29602–29609.
[9] K. Kuwasako, Y.N. Cao, C.P. Chu, S. Iwatsubo, T. Eto, K. Kitamura, Functions of the cytoplasmic tails of the human receptor activity-modifying protein components of calcitonin gene-related peptide and adrenomedullin receptors, J. Biol. Chem. 281 (2006) 7205–7213.
[10] A. Christopoulos, G. Christopoulos, M. Morfis, M. Udawela, M. Laburthe, A. Couvineau, K. Kuwasako, N. Tilakarayne, P.M. Sexton, Novel receptor partners and function of receptor activity-modifying proteins, J. Biol. Chem. 278 (2003) 3293–3297.
[11] K. Kuwasako, K. Kitamura, T. Uemura, Y. Nagoshi, J. Kato, T. Eto, The function of extracellular cysteines in the human adrenomedullin receptor, Hypertens. Res. 26 (2003) S25–S31.
[12] M. Flahaut, B.C. Rossier, D. Firsov, Respective roles of calcitonin receptor-like receptor (CRLR) and receptor activity-modifying proteins (RAMP) in cell surface expression of CRLR/RAMP heterodimeric receptors, J. Biol. Chem. 277 (2002) 14731–14737.
[13] L.M. Itter, F. Luessi, D. Koller, W. Born, J.A. Fischer, R. Muff, Asparate^{69} of the calcitonin-like receptor is required for its functional expression together with receptor-activity-modifying proteins 1 and -2, Biochem. Biophys. Res. Commun. 319 (2004) 1203–1209.
[14] N. Tilakaratne, G. Christopoulos, E.T. Zumpe, S.M. Foord, P.M. Sexton, Amilyn receptor phenotypes derived from human calcitonin receptor/RAMP coexpression exhibit pharmacological differences dependent on receptor isoform and host cell environment, J. Pharmacol. Exp. Ther. 294 (2000) 61–72.
[15] D. Koller, L.M. Ittner, R. Muff, K. Husmann, J.A. Fischer, W. Born, Selective inactivation of adrenomedullin over calcitonin gene-related peptide receptor function by the deletion of amino acids 14–20 of mouse calcitonin-like receptor, J. Biol. Chem. 279 (2004) 20387–20391.
[16] K. Kuwasako, K. Kitamura, Y. Nagoshi, T. Eto, Novel calcitonin-(8-32)-sensitive adrenomedullin receptors derived from co-expression of calcitonin receptor with receptor activity-modifying proteins, Biochem. Biophys. Res. Commun. 301 (2003) 460–464.
[17] M. Morfis, N. Tilakaratne, S.G. Furness, G. Christopoulos, T.D. Werry, A. Christopoulos, P.M. Sexton, Receptor activity-modifying proteins differentially modulates the G protein-coupling efficiency of amylin receptors, Endocrinology 149 (2008) 5423–5431.
[18] K. Kuwasako, Y.N. Cao, Y. Nagoshi, T. Tsuruda, K. Kitamura, T. Eto, Characterization of the human calcitonin gene-related peptide receptor subtypes associated with receptor activity-modifying proteins, Mol. Pharmacol. 65 (2004) 207–213.
[19] T.J. Fitzsimmons, X. Zhao, S.A. Wank, The extracellular domain of receptor activity-modifying protein 1 is sufficient for calcitonin receptor-like receptor function, J. Biol. Chem. 278 (2003) 14313–14320.
[20] L.M. Ittner, D. Koller, R. Muff, J.A. Fischer, W. Born, The N-terminal extracellular domain 23–60 of the calcitonin receptor-like receptor in chimeras with the parathyroid hormone receptor mediates association with receptor activity-modifying protein 1, Biochemistry 44 (2005) 5749–5754.
[21] C.A. Salvatore, J.J. Mallee, I.M. Bell, C.B. Zartman, T.M. Williams, K.S. Koblan, S.A. Kane, Identification and pharmacological characterization of domains involved in binding of CGRP receptor antagonists to the calcitonin-like receptor, Biochemistry 45 (2006) 1881–1887.
[22] J. Lee, J. Gomez-Ramirez, T.H. Johnson, N. Visanji, J.M. Brotchie, Receptor-activity modifying protein 1 expression is increased in the striatum following repeated L-DOPA administration in a 6-hydroxydopamine lesions rat model of Parkinson's disease, Synapse 62 (2008) 310–313.
[23] S.N. Cooray, L. Chan, T.R. Webb, L. Metherell, A.J. Clark, Accessory proteins are vital for the functional expression of certain G protein-coupled receptors, Mol. Cell. Endocrinol. 300 (2009) 17–24.

Hypertension Research (2009) 32, 597–603

www.nature.com/hr

ORIGINAL ARTICLE

Pressure-independent effects of pharmacological stimulation of soluble guanylate cyclase on fibrosis in pressure-overloaded rat heart

Hiroyuki Masuyama[1], Toshihiro Tsuruda[1], Yoko Sekita[1], Kinta Hatakeyama[2], Takuroh Imamura[1], Johji Kato[3], Yujiro Asada[2], Johannes-Peter Stasch[4] and Kazuo Kitamura[1]

Cardiac fibrosis is a hallmark of cardiovascular remodeling associated with hypertension. The purpose of this study was to explore the effect and mechanism of soluble guanylate cyclase (sGC) stimulator BAY 41–2272, leading to intracellular cyclic guanosine monophosphate (cGMP) elevation, on the remodeling process induced by pressure overload. Seven-week-old male Wistar rats with hypertension induced by suprarenal aortic constriction (AC) were treated orally with 2 mg kg^{-1} day^{-1} of BAY 41–2272 for 14 days. BAY 41–2272 had no effects on blood pressure, but decreased AC-induced collagen accumulation in the left ventricle (LV), inhibiting the number of myofibroblasts and gene expressions of transforming growth factor-β1 and type 1 collagen. In addition, the antifibrotic action of BAY 41–2272 was accompanied by reducing AC-induced angiotensin-converting enzyme (ACE) mRNA and its enzymatic activity, and angiotensin II concentration in LV. In cultured cardiac fibroblasts, BAY 41–2272 inhibited ACE synthesis and myofibroblast transformation, accompanied by elevating the intracellular cGMP concentration. These results suggest that sGC stimulator BAY 41–2272 might be effective to reduce fibrosis in hypertensive heart disease by attenuating angiotensin II generation through myofibroblast transformation.
Hypertension Research (2009) **32,** 597–603; doi:10.1038/hr.2009.64; published online 8 May 2009

Keywords: angiotensin; cGMP; fibrosis; soluble guanylate cyclase

INTRODUCTION

Extracellular matrix mainly produced by fibroblasts is essential for organizing an elastic network of cardiocytes in the myocardium, while the structural and functional alteration of these cell types is important in the pathogenesis of hypertensive heart disease, characterized by the left ventricular (LV) hypertrophy and fibrosis.[1–3] As excessive myocardial fibrosis is assumed to be a critical determinant of the deterioration of LV function[4,5] and the cause of arrhythmias,[6] regulating the proliferation and activation of fibroblasts would be an important therapeutic target in the disorder. The renin–angiotensin II (Ang II) system (RAS) is recognized to stimulate fibrosis,[7] whereas the inhibition of either angiotensin-converting enzyme (ACE) or Ang II type 1 receptor has been shown to regress myocardial fibrosis in patients with hypertensive heart disease.[5,8]

Guanylate cyclase is an enzyme that converts guanosine triphosphate to cyclic guanosine monophosphate (cGMP). Both types of guanylate cyclase, particulate guanylate cyclase stimulated by atrial and brain natriuretic peptides,[9–13] and soluble guanylate cyclase (sGC) activated by nitric oxide,[9,14] are reported to attenuate cardiovascular remodeling by elevating intracellular cGMP levels. In an effort to develop agents activating sGC, BAY 41–2272 was identified as an orally active nitric oxide-independent stimulator of the sGC α1-subunit.[15] We and others have shown the beneficial effects of this compound not only on hemodynamics, but also on cardiovascular remodeling.[15–18] As sGC/cGMP activation has been shown to interfere with RAS,[19,20] we tested the hypothesis that the direct stimulation of sGC with BAY 41–2272 could attenuate myocardial fibrosis by inhibiting RAS activation. In this study, we used rats with pressure overload induced by suprarenal aortic constriction (AC), a model of hypertensive heart disease accompanied by fibroblast and RAS activation.[21]

METHODS

This study was performed in accordance with the Animal Welfare Act and approval from the University of Miyazaki Institutional Animal Care and Use Committee (2006-014). This investigation also conformed to the Guide for the Care and Use of Laboratory Animals published by the US National Institutes of Health (NIH Publication No. 85-23, revised 1996).

[1]Department of Internal Medicine, Circulatory and Body Fluid Regulation, Faculty of Medicine, University of Miyazaki, Miyazaki, Japan; [2]Department of Pathology, Faculty of Medicine, University of Miyazaki, Miyazaki, Japan; [3]Frontier Science Research Center, University of Miyazaki, Miyazaki, Japan and [4]PharmD at Cardiovascular Research, Bayer HealthCare, Aprather Weg 18a, Wuppertal, Germany
Correspondence: Dr T Tsuruda, Department of Internal Medicine, Circulatory and Body Fluid Regulation, Faculty of Medicine, University of Miyazaki, 5200 Kihara Kiyotake, Miyazaki 889-1692, Japan.
E-mail: ttsuruda@med.miyazaki-u.ac.jp
Received 22 October 2008; revised 27 February 2009; accepted 7 April 2009; published online 8 May 2009

Animal experiment

Seven-week-old male Wistar rats (Charles River, Yokohama, Japan), weighing 200–250 g, were housed in a temperature and light-controlled room (25 ± 1 °C; 12/12-h light/dark cycle) for 1 week before use, with free access to normal rat chow and water. The rats were divided into three groups: control group (n=11) and two pressure-overloaded groups with (n=21) or without (n=15) BAY 41–2272 treatment. Pressure overload was induced by abdominal AC at the suprarenal level, as described earlier.[22] In brief, a 22-gauge needle was placed adjacent to the abdominal aorta proximal to the renal artery, and ligated tightly around the aorta and the adjacent needle. The needle was then removed, leaving the vessel constricted to the diameter of the needle. The control group underwent identical surgical procedures but without constriction of the aorta. BAY 41–2272 compound, supplied by Bayer HealthCare (Wuppertal, Germany), was given by gastric gavage at a sub-depressor dose of 2 mg kg^{-1} twice a day for 14 days. The dose of BAY 41–2272 was chosen according to our earlier study.[18] The Datascience telemetric system (St Paul, MN, USA) was used to monitor the blood pressure of four unrestricted, conscious rats in each study group, as described earlier.[23] After banding the abdominal aorta, the transmitter catheter (model TA11PA-C40) was inserted into the descending aorta through the left carotid artery, and then the transmitter was implanted in the peritoneal cavity. After surgery, each rat was kept in an individual cage placed on a telemetric receiver pad. Blood pressure and heart rate data were collected for 10 s every 15 min and daily averages were calculated. At day 14, rats were anesthetized with pentobarbital sodium and killed by drawing blood from the thoracic aorta. After the whole heart was weighed, LV was frozen in liquid nitrogen or fixed in 4% paraformaldehyde and embedded in paraffin wax.

Immunohistochemistry and histological analysis

Immunohistochemical staining for α-smooth muscle actin (α-SMA) and ACE were performed as described earlier.[18,24] Slides were stained with mouse anti-α-SMA monoclonal antibody (1:200, Clone 1A4, DakoCytomation, Carpinteria, CA, USA) or rabbit polyclonal antibody against ACE (1:100, Santa Cruz Biotechnology, Santa Cruz, CA, USA) overnight at 4 °C. After the overnight reaction with antibodies, slide sections were incubated with EnVision+ (Dako) for 30 min, visualized with 0.05% 3,3-diaminobenzidine containing hydrogen peroxide, and counterstained with hematoxylin. Myofibroblasts positive for α-SMA were counted at ×200 magnification. To detect collagen fibers, slides were incubated with 0.1% picrosirius red (Direct Red 80, Sigma, St Louis, MO, USA) dissolved in saturated picric acid for 10 min, as described earlier.[18] To measure cardiocyte size, cross-sectional areas of ⩾50 myocardial fibers were measured at the level of nuclei while omitting longitudinally or obliquely sectioned cells as described earlier.[18] Magnitudes of perivascular fibrosis or collagen volume fraction in the interstitial space of myocardial fibers were also determined as described earlier.[18]

Gene expression

Gene expressions of transforming growth factor (TGF)-β1, type 1 collagen and ACE in the LV were measured by real-time quantitative reverse transcription-PCR (ABI Prism 7700 Sequence Detector, Applied Biosystems, Foster City, CA, USA).[18,24] Total RNA Isolation Reagent (Invitrogen, Carlsbad, CA, USA) was used to extract 1 μg of total RNA, which then underwent reverse transcription by means of SuperScript reverse transcriptase (Invitrogen) into cDNA. cDNA was then amplified with oligonucleotide forward and reverse primers and with probes labeled with 6-carboxy-fluorescencein as reporter fluorescence and 6-carboxy-tetramethyl-rhodamine as quencher fluorescence. The oligonucleotide sequences are detailed in earlier reports.[18,24,25] The PCR products were of the expected molecular sizes and the gene expression levels were standardized to those of 18S rRNA.

Cell culture

Cardiac fibroblasts were isolated from 1- to 3-day-old neonatal Wistar rats as described earlier.[18] The cells were grown on culture plates with Dulbecco's modified Eagle's medium containing 10% fetal bovine serum, 10 μg ml^{-1}

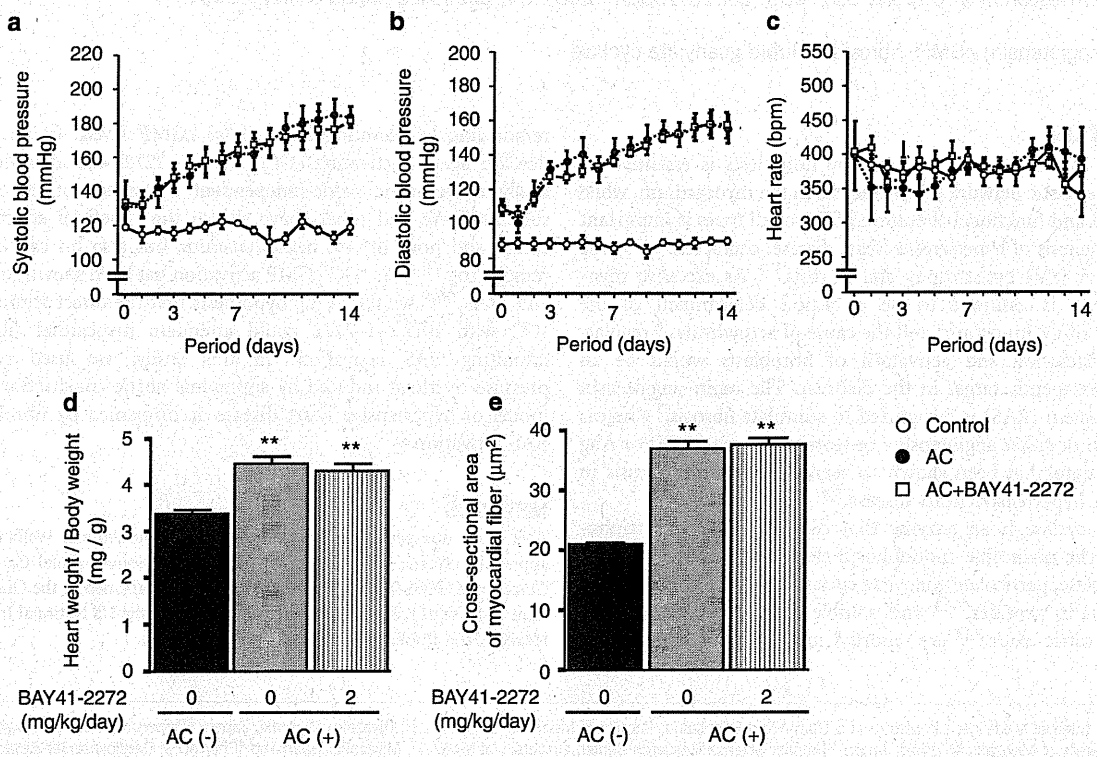

Figure 1 (**a**–**c**) Effects of BAY 41–2272 on systolic (**a**) and diastolic (**b**) blood pressure levels and heart rate (**c**). (**d** and **e**) Effects of BAY41–2272 on heart weight/body weight (**d**) and cross-sectional area of myocardial fibers (**e**). Open circle (○), closed circle (●) and open square (□) indicate the control, aortic constriction (AC) and AC plus BAY 41–2272 treatment, respectively. **P<0.01, compared with the controls. Values are shown as the means ± s.e.m. of four rats (for blood pressure and heart rate) and of 11–21 rats (for heart weight, cross-sectional area of myocardial fibers) in the respective group.

insulin, 5 μg ml^{-1} transferrin and 7 ng ml^{-1} sodium selenite at 37 °C in a 95% air/5% CO_2 humidified atmosphere. After achieving confluence, they were further incubated in serum-free Dulbecco's modified Eagle's medium containing the same additives for 48 h. The cells were then cultured with BAY 41–2272 (10^{-6} and 10^{-5} mol l^{-1}) or non-hydrolysable cGMP analog 8-bromo cGMP (10^{-4} and 10^{-3} mol l^{-1}) (Calbiochem, San Diego, CA, USA) dissolved in dimethyl sulfoxide for a further 24 h. The same volume of dimethyl sulfoxide was added to the control culture medium, and the final concentration of dimethyl sulfoxide did not exceed 0.1% in the culture medium. Thereafter, the cells were collected, and total protein was extracted for western blot as described earlier.[24] In addition, they were extracted to measure ACE activity as described below. The extracted proteins were stored at −80 °C until use.

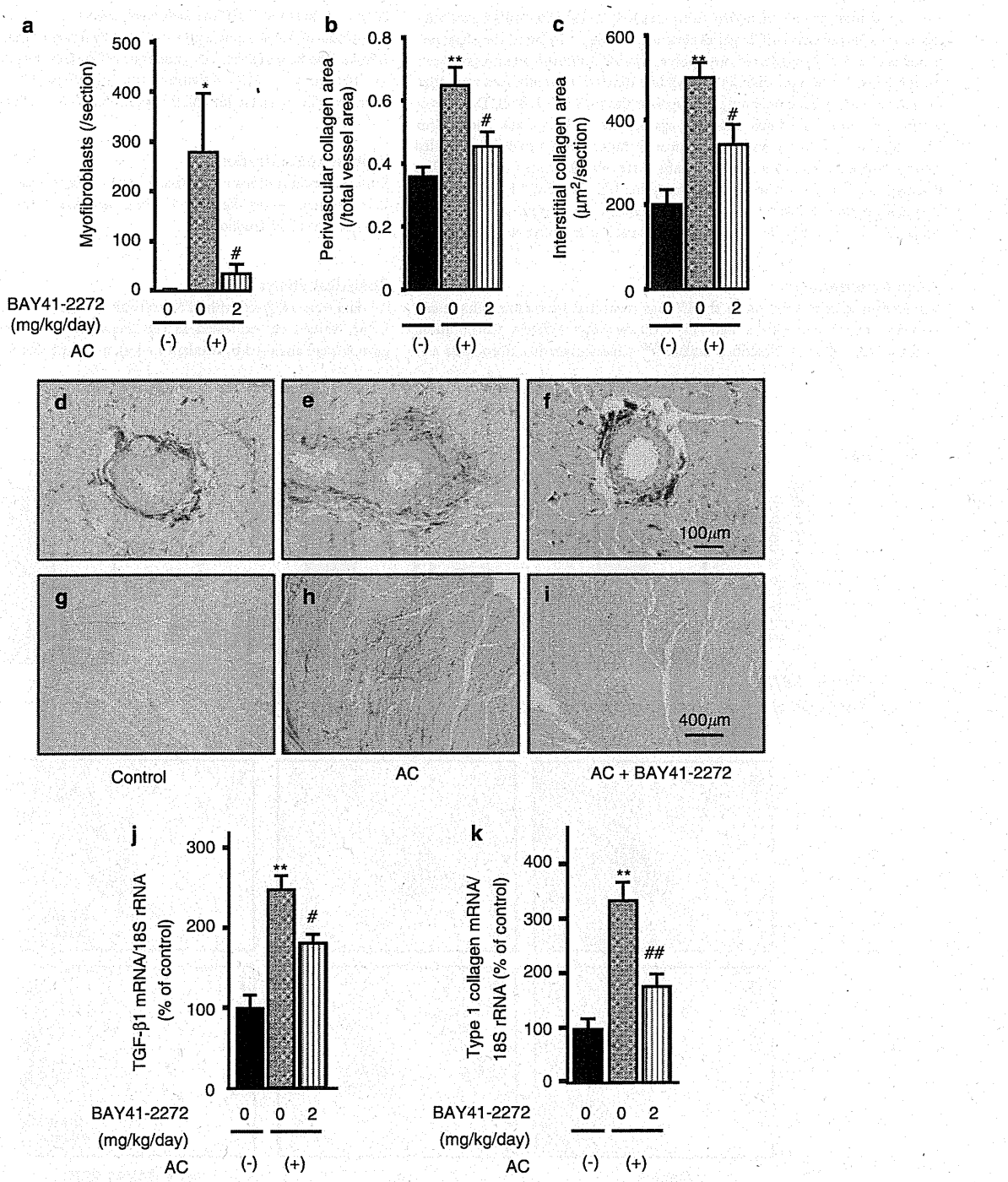

Figure 2 (**a–c**) Effects of BAY 41–2272 on the number of myofibroblasts determined by positive staining for α-SMA (**a**), picrosirius red-positive areas in adventitia of intramyocardial coronary arteries (**b**) and myocardial interstitium (**c**). The panels are representative images of picrosirius red staining in the control (**d** and **g**) and aortic constriction (AC) rats without (**e** and **h**) or with (**f** and **i**) BAY 41–2272 treatment. (**j** and **k**) Effects of BAY 41–2272 on gene expressions for transforming growth factor-β1 (**j**) and type 1 collagen (**k**). Values are shown as the means ± s.e.m. of 9–19 samples in the respective group. $^{*}P<0.05$, $^{**}P<0.01$, compared with the controls; $^{\#}P<0.05$, $^{\#\#}P<0.01$, compared with AC rats without BAY 41–2272 treatment.

Cardiac myocytes were also isolated from 1- to 3-day-old neonatal Wistar rats as described earlier.[26] After culturing the cells under the serum-free Dulbecco's modified Eagle's medium containing 10 μg ml^{-1} insulin, 5 μg ml^{-1} transferrin and 7 ng ml^{-1} sodium selenite for 48 h, BAY 41–2272 (10^{-6} and 10^{-5} mol l^{-1}) was then added to the medium to examine the intracellular cGMP elevation.

Western blot

Denatured total protein obtained from cultured cardiac fibroblasts was subjected to SDS-polyacrylamide gel as described earlier.[12] In brief, the separated proteins electrically transferred onto polyvinylidine difluoride membranes were incubated with 5% skim milk. Polyvinylidine difluoride membranes were then incubated with monoclonal antibody against the α-SMA (1:2000, DakoCytomation) or with polyclonal antibody against the ACE (1:1000, Santa Cruz Biotechnology), followed by incubation with horseradish peroxidase-coupled second antibody. Immunoreactive bands were visualized by the ECL Plus detection kit (GE Healthcare, Buckinghamshire, UK) and band intensities were analyzed densitometrically (Chemi Doc Documentation System, Bio-Rad, Hercules, CA, USA). Coomassie blue staining was used as a protein-loading control.

Radioimmunoassay

Angiotensin II concentration in the LV was measured by radioimmunoassay, following extraction with a Sep-Pak C18 cartridge (Waters Corporation, Milford, MA, USA), as described earlier.[18,27] Cultured cardiac fibroblasts and myocytes treated with or without BAY 41–2272 for 10 min were immediately collected, and the cGMP content was determined using a radioimmunoassay kit (YAMASA Cyclic GMP Assay Kit, Choshi, Japan).[18]

ACE activity

The LV tissues in the respective groups were homogenized in phosphate-buffered saline. Cultured cardiac fibroblasts treated with or without BAY 41–2272 or 8-bromo cGMP for 24 h were collected in 1.8% Triton-X containing phosphate-buffered saline, and were lysed by freezing-thawing three times every 10 min. The homogenized LV tissues or cell lysates were centrifuged at 10 000 *g* for 10 min, 4 °C ACE activity in the supernatants was measured with a commercially available kit (ACE Color, Fujirebio Inc. Tokyo, Japan).

Protein concentration

Protein concentrations of LV tissues and cultured cells were determined with BCA Protein Assay Reagent (Pierce, Rockland, IL, USA), following the manufacturer's instructions.

Statistical analysis

All data were analyzed with SPSS software version 11.0 (SPSS Inc., Chicago, IL, USA). Values are expressed as the means ± s.e.m. Differences between two groups were analyzed by Student's *t*-test, and differences between three groups

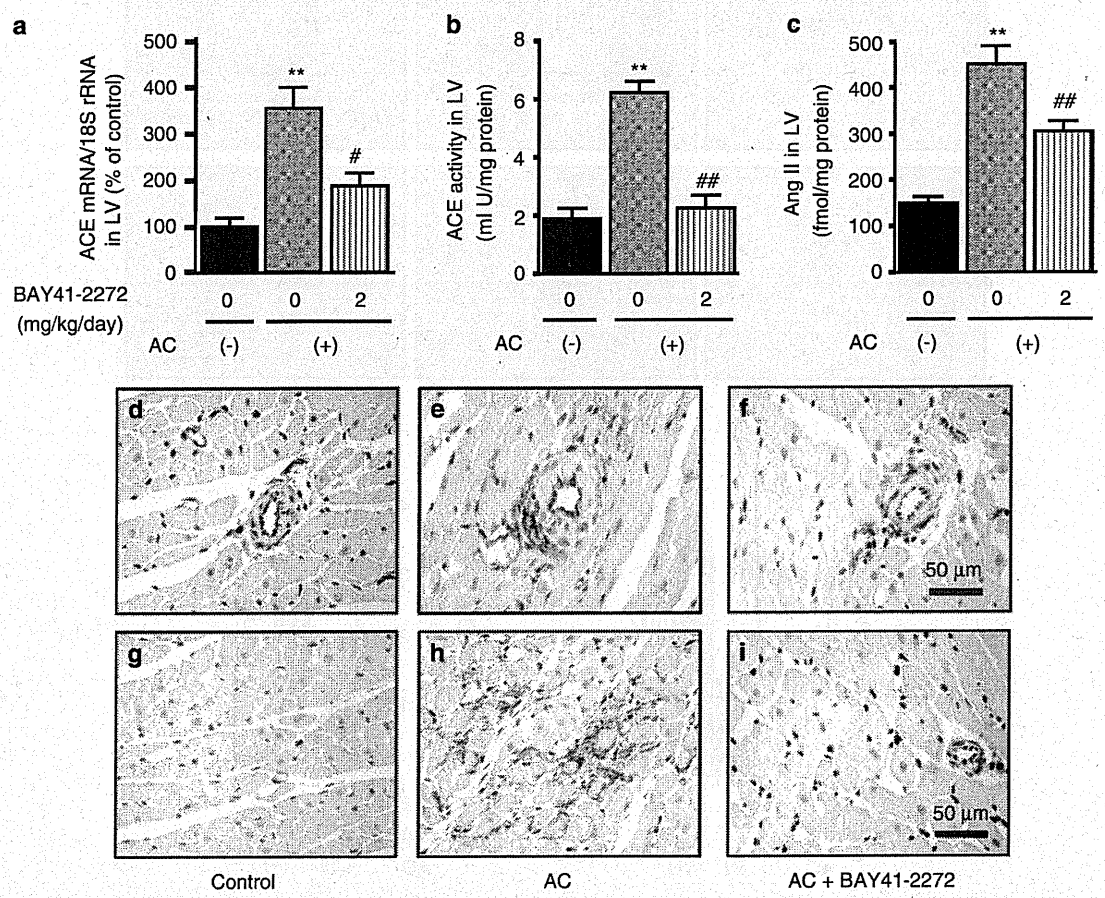

Figure 3 (**a–c**) Effects of BAY 41–2272 on angiotensin-converting enzyme (ACE) mRNA level (**a**), ACE activity (**b**) and Ang II concentration (**c**) in the left ventricle (LV). The panels are representative images of ACE immunoreactivity in the control (**d** and **g**) and aortic constriction (AC) rats without (**e** and **h**) or with (**f** and **i**) BAY 41–2272 treatment. Bar: 50 μm. Values are shown as the means ± s.e.m. of 11–16 in the respective group. $^{**}P<0.01$, compared with the controls; $^{\#}P<0.05$, $^{\#\#}P<0.01$, compared with AC rats without BAY 41–2272.

were assessed using one-way analysis of variance followed by Scheffé's test, and statistical significance was accepted at $P<0.05$. In western blot analysis, standard curves were made by serial dilution of samples, and bands on gels were quantified based on the optical density.

RESULTS

Hemodynamics, heart weight and cardiocyte size

Figures 1a–c show the blood pressure and heart rate in the controls and AC rats with or without BAY 41–2272 treatment. AC progressively raised systolic and diastolic blood pressure levels; however, BAY 41–2272 had no effect on the AC-induced elevation of blood pressure. Heart rate was unchanged in the respective groups. As shown in Figures 1d and e, AC significantly ($P<0.01$) increased the ratio of heart weight to body weight (HW/BW) and the cross-sectional area of myocardial fibers, compared with the controls; however, BAY 41–2272 did not affect the AC-induced increase in HW/BW and cardiocyte size.

Myofibroblasts and collagen deposition

Figures 2a–c show that AC increased the number of myofibroblasts and collagen depositions in the perivascular and the interstitial areas of LV, but BAY 41–2272 administration significantly ($P<0.05$) decreased them by 88, 30 and 46%, respectively. Representative collagen deposition in the respective groups are shown in Figures 2d–i. As shown in Figures 2j and k, BAY 41–2272 administration significantly ($P<0.05$) attenuated the AC-induced elevation of gene expressions of TGF-β1 and type 1 collagen.

Ang II synthesis

Figure 3a and b show that AC significantly ($P<0.01$) increased the gene expression and activity of ACE in LV, but BAY 41–2272 significantly ($P<0.01$) reduced them by 47 and 64%, respectively. Figure 3c shows that BAY 41–2272 administration significantly ($P<0.01$) attenuated the AC-induced increase of Ang II concentration in LV by 36%. As shown in Figures 3d–i, ACE immunoreactivity

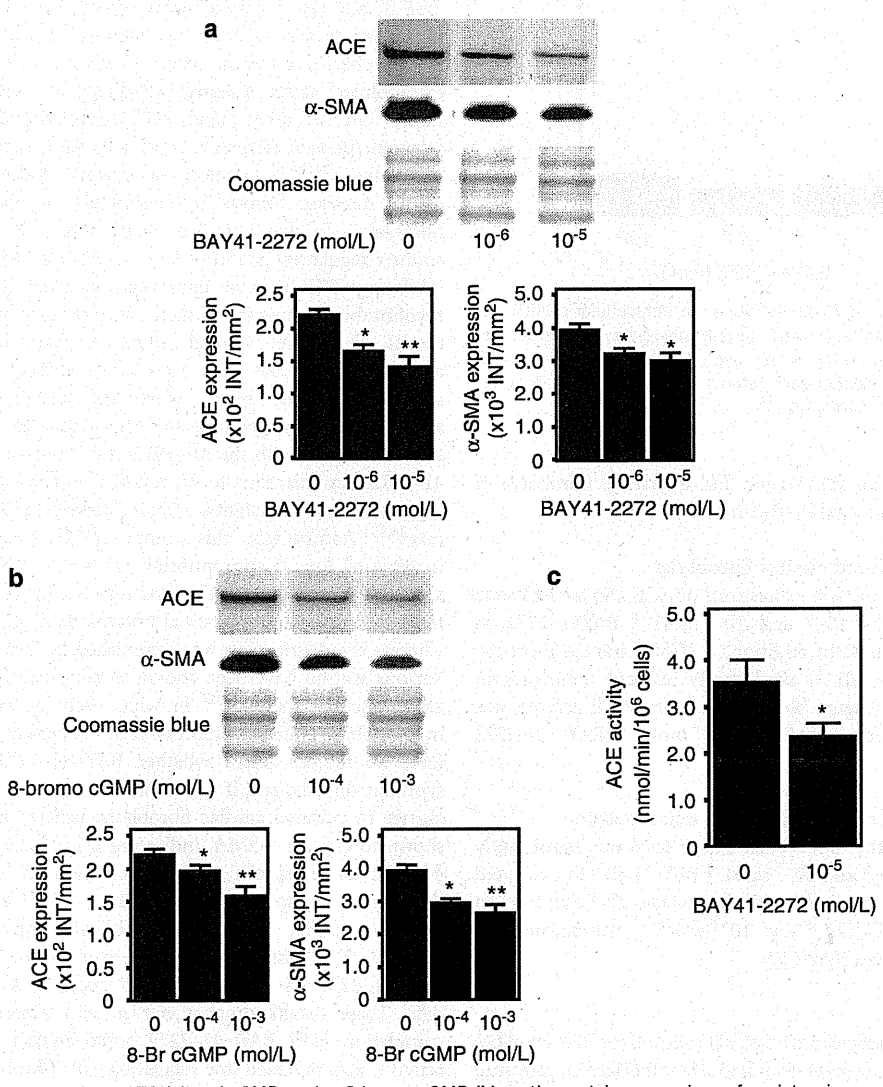

Figure 4 (**a** and **b**) Effects of BAY 41–2272 (**a**) and cGMP analog 8-bromo cGMP (**b**) on the protein expressions of angiotensin-converting enzyme (ACE) and α-smooth muscle actin (α-SMA) in cultured cardiac fibroblasts. (**c**) Effect of BAY 41–2272 on ACE activity in cell lysates. The panels show representative images of western blotting, and values are shown as the means ± s.e.m. of 4–6 (**a** and **b**), 9 and 11 (**c**) samples examined. *$P<0.05$, **$P<0.01$, compared with control cells without either BAY 41–2272 or 8-bromo cGMP. Coomassie blue was used as the protein loading control.

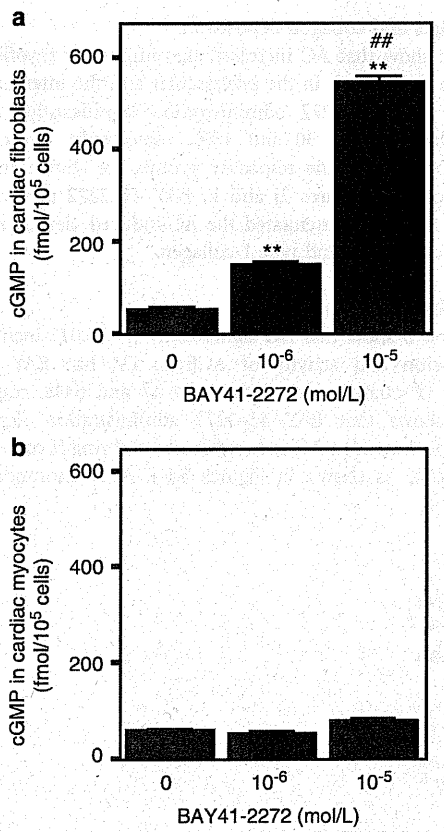

Figure 5 (**a** and **b**) Effect of BAY 41–2272 on the intracellular cGMP level in cultured cardiac fibroblasts (**a**) and cardiac myocytes (**b**). Values are shown as the means ± s.e.m. of 4 (**a**) and 8 (**b**) samples examined. $^{**}P<0.01$, compared with control cells without BAY 41–2272, $^{\#\#}P<0.01$, compared with 10^{-6} mol l^{-1} BAY 41–2272.

increased to localize in the perivascular and interstitial fibroblasts of AC rats, while it was decreased by treatment.

ACE and α-SMA in cultured cardiac fibroblasts

Figure 4a shows that the protein expressions of ACE and α-SMA were significantly decreased by 10^{-6} and 10^{-5} mol l^{-1} BAY41–2272 in cultured cardiac fibroblasts. In addition, a cGMP analog, 8-bromo cGMP (10^{-4} and 10^{-3} mol l^{-1}) significantly reduced these protein expressions in the cells (Figure 4b). Furthermore, ACE activity was significantly ($P<0.05$) decreased by 10^{-5} mol l^{-1} BAY 41–2272 (Figure 4c).

cGMP level in cultured cardiac fibroblasts and myocytes

As shown in Figure 5a, the intracellular cGMP level was significantly ($P<0.01$) elevated by 10^{-5} and 10^{-6} mol l^{-1} BAY 41–2272 in cultured cardiac fibroblasts. On the other hand, the change of cGMP level in response to BAY 41–2272 (10^{-5} and 10^{-6} mol l^{-1}) was minimal in cultured cardiac myocytes (Figure 5b).

DISCUSSION

This study shows the beneficial action of sGC stimulator BAY 41–2272 on attenuating fibrosis in a hypertrophied heart induced by pressure overload, independently of blood pressure. In addition, the inhibition of myofibroblast transformation and RAS activation appear be involved in this mechanism.

We have earlier reported that the depressor dose of sGC stimulation with BAY 41–2272 was effective to decrease cardiocyte hypertrophy and fibrosis, but the sub-depressor dose exhibited to decrease fibrosis without reducing cardiocyte hypertrophy in the Ang II-induced hypertensive model.[18] This study was consistent to show that the sub-depressor dose of this compound decreased the fibrosis without altering cardiocyte hypertrophy defined by HW/BW and cross-sectional area of myocardial fiber in the model of pressure overload. Although precise mechanisms by which the sub-depressor dose of sGC stimulation facilitates to decrease fibrosis remain to be elucidated, we might speculate the discrepancy between fibrosis and heart weight in response to the sGC stimulation by the following two reasons: (1) mechanical load is a major contributor to cardiocyte hypertrophy,[7] and therefore the sub-depressor dose BAY 41–2272 was insufficient to influence the cardiocyte hypertrophy induced by pressure-overload; (2) *in vitro* experiment suggests that cardiac fibroblasts appear to be more feasible to exert cGMP elevation than cardiac myocytes by the compound. Using a sub-depressor dose of BAY 41–2272, the attenuation of fibrosis by this compound was associated with the reduction of TGF-β1 and type 1 collagen expressions. TGF-β1 is reported to be an important trigger to exert the phenotypic change of fibroblasts to myofibroblasts, a central player in exaggerating the production of extracellular matrix proteins, including type 1 collagen and fibronection.[28] On the other hand, sGC stimulation has been shown to attenuate/prevent fibrosis in various organs, such as the lungs, liver and kidneys;[20,29–31] therefore, we examined whether this compound would decrease fibrosis by inhibiting the phenotypic change in fibroblasts. In line with our hypothesis, this study suggests the counter-regulatory action of BAY 41–2272 on the fibrotic process by inhibiting TGF-β1 gene expression, concomitant with attenuating myofibroblast transformation in the pressure-overloaded heart. The model of pressure overload induced by constricting the suprarenal abdominal aorta has been reported to exhibit the substantial RAS activation in the heart, while the circulating RAS was less affected,[21,22,32,33] suggesting that Ang II generation in the LV is likely to be associated with the progression of fibrosis. It is noted that BAY 41–2272 administration to AC rats has been shown to lower ACE gene expression and its activity, a main enzyme for Ang II generation in rats.[34,35] Accordingly, this compound decreased the AC-induced increase of Ang II concentration in the LV. Consistent with earlier reports,[34,35] ACE immunoreactivity showed increased distribution in the perivascular and interstitial fibroblasts of pressure-overloaded LV, whereas the distribution was diminished by BAY 41–2272 treatment. Various stimuli have been shown to stimulate ACE synthesis in the cardiovascular system,[36,37] in which activity was increased during myofibroblast transformation in cultured cardiac fibroblasts.[38] Therefore, we further tested whether BAY 41–2272 could affect ACE synthesis directly, and if so, whether it is associated with phenotypic change in cultured cardiac fibroblasts. Isolated fibroblasts have been shown to express α-SMA, indicating myofibroblasts. As shown, BAY 41–2272 decreased the protein expressions of ACE and α-SMA in these cells, accompanied by intracellular cGMP elevation. In addition, 8-bromo cGMP, an analog of cGMP, mimicked the effect of BAY 41–2272, inhibiting these expressions. More importantly, BAY 41–2272 has been shown to decrease ACE activity in these cells. These results support our *in vivo* observations, which sGC stimulation with BAY 41–2272 could inhibit ACE synthesis and activity, accompanied by regulating the fibroblast phenotype. We have earlier reported that BAY 41–2272 was capable of inhibiting cardiac fibroblast proliferation under Ang II stimulation.[18] Taken together, we propose that pharmacological intervention with the orally

effective sGC stimulator BAY 41–2272 points to an antifibrotic action, in which the inhibition of myofibroblasts transformation and Ang II synthesis might induce specific benefits against the development of hypertensive heart disease.

In summary, sGC stimulation with BAY 41–2272 attenuated cardiac fibrosis independently of blood pressure, and the inhibition of myofibroblast transformation and Ang II synthesis appear to be the potential mechanisms involved. Thus, our present study supports the sGC-cGMP-dependent beneficial action against adverse cardiovascular remodeling associated with hypertension. Further studies are warranted to clarify the long-term benefit and safety of this compound for future's clinical practice.

CONFLICT OF INTEREST

Toshihiro Tsuruda received a research grant from Bayer HealthCare. BAY 41–2272 was synthesized at Bayer HealthCare as a research tool but not for use in humans.

ACKNOWLEDGEMENTS

We thank Ms Ritsuko Sotomura for technical assistance. This study was supported by Grants-in-aid for Scientific Research (C) (20590830) from the Ministry of Education, Culture, Sports, Science, and Technology, Japan and from Bayer HealthCare.

1 Levy D, Larson MG, Vasan RS, Kannel WB, Ho KK. The progression from hypertension to congestive heart failure. *JAMA* 1996; **275**: 1557–1562.
2 Kai H, Kuwahara F, Tokuda K, Imaizumi T. Diastolic dysfunction in hypertensive hearts: roles of perivascular inflammation and reactive myocardial fibrosis. *Hypertens Res* 2005; **28**: 483–490.
3 Diamond JA, Phillips RA. Hypertensive heart disease. *Hypertens Res* 2005; **28**: 191–202.
4 Müller-Brunotte R, Kahan T, López B, Edner M, González A, Díez J, Malmqvist K. Myocardial fibrosis and diastolic dysfunction in patients with hypertension: results from the Swedish Irbesartan Left Ventricular Hypertrophy Investigation versus Atenolol (SILVHIA). *J Hypertens* 2007; **25**: 1958–1966.
5 Díez J, Querejeta R, López B, González A, Larman M, Martínez Ubago JL. Losartan-dependent regression of myocardial fibrosis is associated with reduction of left ventricular chamber stiffness in hypertensive patients. *Circulation* 2002; **105**: 2512–2517.
6 McLenachan JM, Dargie HJ. Ventricular arrhythmias in hypertensive left ventricular hypertrophy. Relationship to coronary artery disease, left ventricular dysfunction, and myocardial fibrosis. *Am J Hypertens* 1990; **3**: 735–740.
7 Weber KT. Fibrosis and hypertensive heart disease. *Curr Opin Cardiol* 2000; **15**: 264–272.
8 Brilla CG, Funck RC, Rupp H. Lisinopril-mediated regression of myocardial fibrosis in patients with hypertensive heart disease. *Circulation* 2000; **102**: 1388–1393.
9 Calderone A, Thaik CM, Takahashi N, Chang DL, Colucci WS. Nitric oxide, atrial natriuretic peptide, and cyclic GMP inhibit the growth-promoting effects of norepinephrine in cardiac myocytes and fibroblast. *J Clin Invest* 1998; **101**: 812–818.
10 Mori T, Chen YF, Feng JA, Hayashi T, Oparil S, Perry GJ. Volume overload results in exaggerated cardiac hypertrophy in the atrial natriuretic peptide knockout mouse. *Cardiovasc Res* 2004; **61**: 771–779.
11 Cao L, Gardner DG. Natriuretic peptides inhibit DNA synthesis in cardiac fibroblasts. *Hypertension* 1995; **25**: 227–234.
12 Tsuruda T, Boerrigter G, Huntley BK, Noser JA, Cataliotti A, Costello-Boerrigter LC, Chen HH, Burnett Jr JC. Brain natriuretic peptide is produced in cardiac fibroblasts and induces matrix metalloproteinases. *Circ Res* 2002; **91**: 1127–1134.
13 Tamura N, Ogawa Y, Chusho H, Nakamura K, Nakao K, Suda M, Kasahara M, Hashimoto R, Katsuura G, Mukoyama M, Itoh H, Saito Y, Tanaka I, Otani H, Katsuki M. Cardiac fibrosis in mice lacking brain natriuretic peptide. *Proc Natl Acad Sci USA* 2000; **97**: 4239–4244.
14 Kim NN, Villegas S, Summerour SR, Villarreal FJ. Regulation of cardiac fibroblast extracellular matrix production by bradykinin and nitric oxide. *J Mol Cell Cardiol* 1999; **31**: 457–466.
15 Stasch JP, Becker EM, Alonso-Alija C, Apeler H, Denbowsky K, Feurer A, Gerzer R, Minuth T, Perzborn E, Pleiβ U, Schröder H, Schroeder W, Stahl E, Steinke W, Straub A, Schramm M. NO-independent regulatory site on soluble guanylate cyclase. *Nature* 2001; **410**: 212–215.
16 Boerrigter G, Costello-Boerrigter LC, Cataliotti A, Tsuruda T, Harty GJ, Lapp H, Stasch JP, Burnett Jr JC. Cardiorenal and humoral properties of a novel direct soluble guanylate cyclase stimulator BAY41–2272 in experimental congestive heart failure. *Circulation* 2003; **107**: 686–689.
17 Evgenov OV, Ichinose F, Evgenov NV, Gnoth MJ, Falkowski GE, Chang Y, Bloch KD, Zapol WM. Soluble guanylate cyclase activator reverses acute pulmonary hypertension and augments the pulmonary vasodilator response to inhaled nitric oxide in awake lambs. *Circulation* 2004; **110**: 2253–2259.
18 Masuyama H, Tsuruda T, Kato J, Imamura T, Asada Y, Stasch JP, Kitamura K, Eto T. Soluble guanylate cyclase stimulation on cardiovascular remodeling in angiotensin II-induced hypertensive rats. *Hypertension* 2006; **48**: 972–978.
19 Yan C, Kim D, Aizawa T, Berk BC. Functional interplay between angiotensin II and nitric oxide: cyclic GMP as a key mediator. *Arterioscler Thromb Vasc Biol* 2003; **23**: 26–36.
20 Dunkern TR, Feurstein D, Rossi GA, Sabatini F, Hatzelmann A. Inhibition of TGF-β induced lung fibroblast to myofibroblast conversion by phosphodiesterase inhibiting drugs and activators of soluble guanylyl cyclase. *Eur J Pharmacol* 2007; **572**: 12–22.
21 Kuwahara F, Kai H, Tokuda K, Kai M, Takeshita A, Egashira K, Imaizumi T. Transforming growth factor-β function blocking prevents myocardial fibrosis and diastolic dysfunction in pressure-overloaded rats. *Circulation* 2002; **106**: 130–135.
22 Hirano S, Imamura T, Onitsuka H, Matsuo T, Kitamura K, Koiwaya Y, Eto T. Rapid increase in cardiac adrenomedullin gene expression caused by acute pressure overload: effect of the renin-angiotensin system on gene expression. *Circ J* 2002; **66**: 397–402.
23 Tonkiss J, Trzcivska M, Galler JR, Ruiz-Opazo N, Herrera VLM. Prenatal malnutrition-induced changes in blood pressure. Dissociation of stress and nonstress responses using radiotelemetry. *Hypertension* 1998; **32**: 108–114.
24 Tsuruda T, Kato J, Hatakeyama K, Masuyama H, Cao YN, Imamura T, Kitamura K, Asada Y, Eto T. Antifibrotic effect of adrenomedullin on coronary adventitia in angiotensin II-induced hypertensive rats. *Cardiovasc Res* 2005; **65**: 921–929.
25 Naito Y, Tsujino T, Fujioka Y, Ohyanagi M, Iwasaki T. Augmented diurnal variations of the cardiac renin-angiotensin system in hypertensive rats. *Hypertension* 2002; **40**: 827–833.
26 Tsuruda T, Kato J, Kitamura K, Kuwasako K, Imamura T, Koiwaya Y, Tsuji T, Kangawa K, Eto T. Adrenomedullin: a possible autocrine or paracrine inhibitor of hypertrophy of cardiomyocytes. *Hypertension* 1998; **31**: 505–510.
27 Nagata S, Kato J, Sasaki K, Minamino N, Eto T, Kitamura K. Isolation and identification of proangiotensin-12, a possible component of the renin-angiotensin system. *Biochem Biophys Res Commun* 2006; **350**: 1026–1031.
28 Powell DW, Mifflin RC, Valentich JD, Crowe SE, Saada JI, West AB. Myofibroblasts. I. Paracrine cells important in health and disease. *Am J Physiol* 1999; **277**: C1–C9.
29 Wang Y, Krämer S, Loof T, Martini S, Kron S, Kawachi H, Shimizu F, Neumayer HH, Peters H. Enhancing cGMP in experimental progressive renal fibrosis: soluble guanylate cyclase stimulation vs phosphodiesterase inhibition. *Am J Physiol Renal Physiol* 2006; **290**: F167–F176.
30 Kalk P, Godes M, Relle K, Rothkegel C, Hucke A, Stasch JP, Hocher B. NO-independent activation of soluble guanylate cyclase prevents disease progression in rats with 5/6 nephrectomy. *Br J Pharmacol* 2006; **148**: 853–859.
31 Knorr A, Hirth-Dietrich C, Alonso-Alija C, Härter M, Hahn M, Keim Y, Wunder F, Stasch JP. Nitric oxide-independent activation of soluble guanylate cyclase by BAY 60–2770 in experimental liver fibrosis. *Arzneimittelforschung* 2008; **58**: 71–80.
32 Tokuda K, Kai H, Kuwahara F, Yasukawa H, Tahara N, Kudo H, Takemiya K, Koga M, Yamamoto T, Imaizumi T. Pressure-independent effects of angiotensin II on hypertensive myocardial fibrosis. *Hypertension* 2004; **43**: 499–503.
33 Kobayashi S, Yano M, Kohno M, Obayashi M, Hisamatsu Y, Ryoke T, Ohkusa T, Yamakawa K, Matsuzaki M. Influence of aortic impedance on the development of pressure-overload left ventricular hypertrophy in rats. *Circulation* 1996; **94**: 3362–3368.
34 Kurosawa Y, Katoh M, Doi H, Narita H. Tissue angiotensin-converting enzyme activity plays an important role in pressure overload-induced cardiac fibrosis in rats. *J Cardiovasc Pharmacol* 2002; **39**: 600–609.
35 de Lannoy LM, Schuijt MP, Saxena PR, Schalekamp MA, Danser AH. Angiotensin converting enzyme is the main contributor to angiotensin I-II conversion in the interstitium of the isolated perfused rat heart. *J Hypertens* 2001; **19**: 959–965.
36 Barreto-Chaves ML, Anéas I, Krieger JE. Glucocorticoid regulation of angiotensin-converting enzyme in primary culture of adult cardiac fibroblasts. *Am J Physiol Regul Integr Comp Physiol* 2001; **280**: R25–R32.
37 Saijonmaa O, Nyman T, Kosonen R, Fyhrquist F. Upregulation of angiotensin-converting enzyme by vascular endothelial growth factor. *Am J Physiol Heart Circ Physiol* 2001; **280**: H885–H891.
38 Petrov VV, Fagard RH, Lijnen PJ. Transforming growth factor-β1 induces angiotensin-converting enzyme synthesis in rat cardiac fibroblasts during their differentiation to myofibroblasts. *J Renin Angiotensin Aldosterone Syst* 2000; **1**: 342–352.

Regulatory Peptides 158 (2009) 127–131

Contents lists available at ScienceDirect

Regulatory Peptides

journal homepage: www.elsevier.com/locate/regpep

Increased plasma levels of the mature and intermediate forms of adrenomedullin in obesity

Ikuo Nomura [a], Johji Kato [b,*], Mariko Tokashiki [a], Kazuo Kitamura [a]

[a] Department of Internal Medicine, Circulatory and Body Fluid Regulation, Faculty of Medicine, University of Miyazaki, Kiyotake, Miyazaki 889-1692, Japan
[b] Frontier Science Research Center, University of Miyazaki, 5200 Kihara, Kiyotake, Miyazaki 889-1692, Japan

ARTICLE INFO

Article history:
Received 23 April 2009
Received in revised form 20 June 2009
Accepted 16 August 2009
Available online 23 August 2009

Keywords:
Body mass index
Insulin sensitivity
Metabolic disorder

ABSTRACT

Adrenomedullin (AM) is a cardiovascular protective peptide produced in various organs and tissues including adipose tissue. In the present study, we measured the plasma AM levels of subjects with or without obesity by two assay methods to separately evaluate the biologically active AM–NH_2 and the intermediate form of AM–glycine (AM–Gly). We measured the total AM and AM–NH_2 levels of plasma in 52 obese and 172 non-obese residents of a Japanese community, who received regular health check-ups and had no overt cardiovascular disease. AM–Gly values were obtained by subtracting AM–NH_2 levels from those of total AM. Both the AM–NH_2 and AM–Gly levels of the subjects with obesity were higher than those without obesity, and significant relationships were noted between body mass index (BMI) and the plasma levels of the two molecular forms of AM in a simple regression analysis. Moreover, the significant factors identified by multivariate analyses were BMI and serum triglyceride for AM–NH_2 and diastolic blood pressure, insulin, high-density lipoprotein-cholesterol, and plasma renin activity for AM–Gly. These results suggest active roles for the two molecular forms of AM in metabolic disorders associated with obesity in subjects without overt cardiovascular disease.

1. Introduction

Consisting of 52 amino-acid residues, adrenomedullin (AM) is a biologically active peptide that exerts a wide range of actions including vasodilatation, improvement of vascular endothelial function, inhibition of cardiovascular remodeling, modulation of adipogenesis, and alleviation of insulin resistance [1–7]. Although it was initially isolated from pheochromocytoma tissue, the AM peptide is produced in various organs such as the adrenal medulla, heart, blood vessels, and adipose tissue [1–9]. AM also circulates in human blood, and plasma AM levels were found to be elevated in patients with hypertension, obesity, heart failure, acute myocardial infarction, and atherosclerotic vascular diseases [2–4,10–13]. Based on its biological actions, AM is assumed to participate in mechanisms that act against the development or progression of metabolic or cardiovascular diseases. In the biosynthesis of AM peptide, the intermediate form AM–glycine (AM–Gly) is processed from the AM precursor proAM, a 126 amino-acid peptide, and then the biologically active mature form of AM–NH_2 is produced by the action of amidation enzymes [2–4]. We previously reported that AM in the human blood consists of two molecular forms, the mature and intermediate AM peptides [14]. There have been a number of reports on AM measurement in human plasma; however, the assay methods used in most of these studies were unable to measure the mature and intermediate AM levels separately [2–4,14]. In the present study, we measured plasma AM levels with two types of immunoreactive radiometric assays (IRMA) to detect AM–NH_2 and AM–Gly in non-obese and obese residents of a Japanese community without overt cardiovascular disease. We then compared these AM levels with other clinical parameters, to study the pathophysiological role of AM in obesity-related metabolic disorders.

2. Materials and methods

2.1. Study subjects and protocol

Local residents of the Kiyotake area, Miyazaki, Japan, who underwent an annual regular health check-up in 2007 were examined for this study (81 males and 143 females; 60.8 ± 9.8 years, mean ± SD). Upon visiting the community center of Kiyotake town, the medical history of the subjects was taken by nurses and confirmed by physicians. The subjects enrolled were determined to have no overt cardiovascular diseases such as ischemic heart disease, congestive heart failure, or stroke from their medical history and physical examination, and those given glucose-lowering agents for diabetes mellitus were excluded from this study to allow the precise evaluation of insulin-sensitivity. Obesity was defined as a body mass index (BMI) of 25 Kg/m^2 or higher, according to the criteria of the Japan Society for the Study of Obesity [15]. Blood pressure was measured with an oscillometric automatic device (BP-103iII, Colin, Japan) in a sitting

* Corresponding author. Tel.: +81 985 85 9718; fax: +81 985 85 6596.
E-mail address: jkjpn@med.miyazaki-u.ac.jp (J. Kato).

0167-0115/$ – see front matter © 2009 Elsevier B.V. All rights reserved.
doi:10.1016/j.regpep.2009.08.003

Table 1
The basal profile of the subjects examined in this study.

	Non-obese	Obese
Male/female (*n*)	57/115	24/28
Age (year)	60.5 ± 9.7	61.5 ± 10.3
SBP (mmHg)	123 ± 18	134 ± 17**
DBP (mmHg)	74 ± 11	79 ± 10**
BMI (kg/m^2)	21.4 ± 2.0	27.5 ± 3.3**
Serum creatinine (mg/dl)	0.71 ± 0.14	0.76 ± 0.19

SBP and DBP: systolic and diastolic blood pressure; BMI: body mass index; mean ± SD; **$P<0.01$.

Table 2
Metabolic and humoral factors.

	Non-obese	Obese
Fasting blood glucose (mg/dl)	96 ± 16	106 ± 26**
Insulin (μIU/ml)	4.3 ± 2.0	8.9 ± 5.4**
HOMA index	1.04 ± 0.52	2.47 ± 2.40**
Cholesterol (mg/dl)	211 ± 32	213 ± 32
HDL-cholesterol (mg/dl)	64 ± 13	56 ± 13**
Triglyceride (mg/dl)	97 ± 54	123 ± 86**
Plasma renin activity (ng/ml/h)	0.87 ± 0.64	0.88 ± 0.54
Plasma aldosterone (pg/ml)	87 ± 45	92 ± 40

HOMA: homeostasis model assessment; HDL: high-density lipoprotein; mean ± SD; **$P<0.01$.

position by experienced nurses, and then blood was drawn from an antecubital vein after overnight fasting. To measure the total and mature AM levels in plasma, blood was collected in tubes with 1.0 mg/mL

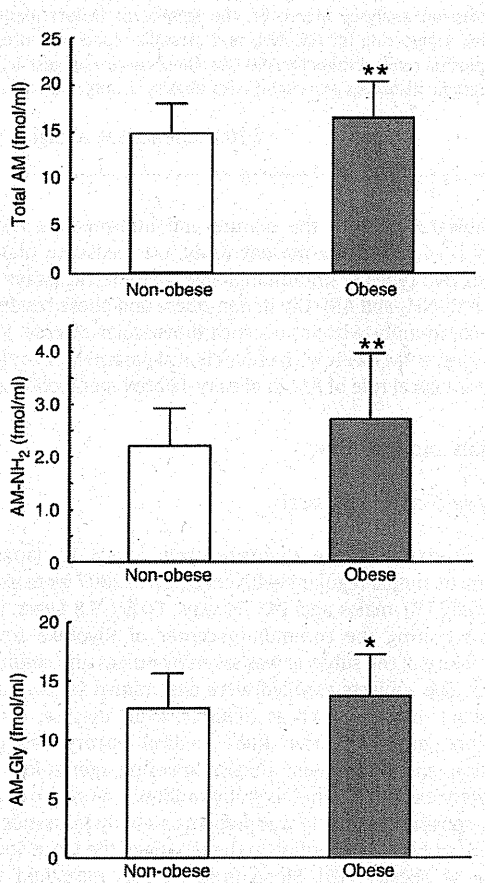

Fig. 1. Plasma levels of total AM, AM–NH_2, and AM–Gly in non-obese and obese subjects. The data are shown as means ± SD. *$P<0.05$, **$P<0.01$, vs. non-obese subjects.

Table 3
Coefficients of correlation obtained by simple regression analysis.

	AM–NH_2	AM–Gly
Basal parameters		
Age	0.142*	n.s.
BMI	0.222**	0.211**
SBP	0.152*	0.259**
DBP	0.149*	0.296**
Serum creatinine	n.s.	0.181**
Metabolic or humoral parameters		
Insulin	n.s.	0.313**
HOMA index	n.s.	0.293**
HDL-cholesterol	n.s.	−0.266**
Triglycerides	0.198**	0.273**
Plasma renin activity	n.s.	0.199**

The abbreviations are listed in Tables 1 and 2. *$P<0.05$, **$P<0.01$, n.s. = not significant.

of EDTA-2Na and 500 kallikrein inhibitory units (KIU)/mL of aprotinin. Plasma was obtained by centrifugation at 3000 rpm for 10 min at 4 °C and stored at −40 °C until the assay.

This study was approved by the Review Committee for Cooperative and Commissioned Research and the Ethics Committee of the University of Miyazaki Faculty of Medicine. All subjects examined gave their written informed consent before participating in this study.

2.2. Assay procedures

Total and mature AM levels were measured by AM RIA and AM mature RIA (Shionogi Pharmaceutical Co., Ltd., Osaka, Japan), respectively [16,17], and values for the intermediate form AM–Gly were obtained by subtracting the plasma levels of AM–NH_2 from those of total AM. The details of these assays are described in the original reports by Ohta et al. and those of others [7,16,17]. Plasma

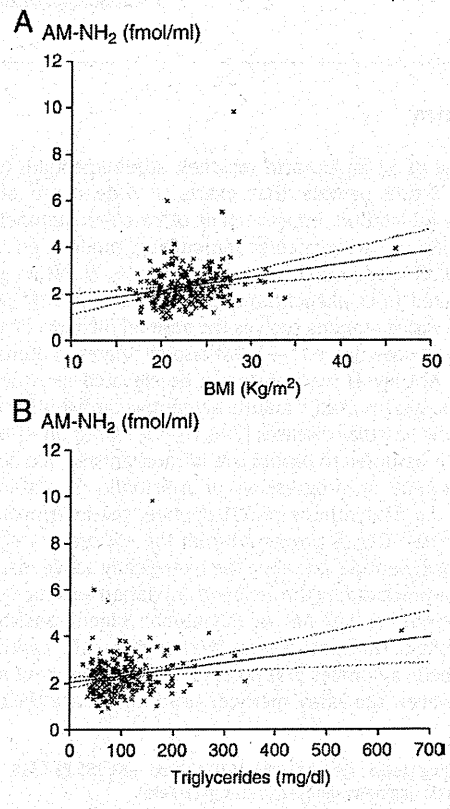

Fig. 2. Relationships between the AM–NH_2 and BMI (A) or serum triglyceride level (B). Regression lines and 95% confidence limits are shown on each graph.

renin activity and aldosterone concentration were determined by radioimmunoassays as previously reported [11], and serum insulin level was measured by an enzyme immunoassay. Serum lipid and glucose levels were measured with an automatic analyzer (OLYMPUS AU2700, OLYMPUS, Tokyo, Japan), and serum creatinine levels were determined by an enzymatic method.

2.3. Statistical analysis

All the data were analyzed with SPSS software version 17.0 (SPSS Inc., Chicago, IL, USA). Comparisons between two groups were assessed by the unpaired *t*-test or chi-squared test, and correlations between two parameters were tested by simple regression analysis. The relationships were further analyzed by multiple regression analysis with a step-wise method to identify the factor(s) independently associated with the plasma levels of AM–NH_2 and AM–Gly. In this multivariate analysis, the basal or metabolic factors that were found to be significant by simple regression were used as independent covariates. All the data are expressed as means ± S.D., and *P* values of less than 0.05 were considered to be significant.

3. Results

In a comparison of the basal clinical data from the non-obese and obese residents (Table 1), no significant differences were noted in gender, age, or serum creatinine levels, while both the systolic and diastolic blood pressure (SBP and DBP) levels of the obese subjects were higher than those of the non-obese subjects. The results of the measurement of metabolic and humoral factors are shown in Table 2, where obesity-related metabolic parameters such as the blood levels of fasting glucose, insulin, high-density lipoprotein-cholesterol (HDL-cholesterol), triglycerides, and the homeostasis model assessment (HOMA) index of the subjects with obesity are shown to be higher than those without obesity, but this was not the case for serum total cholesterol level, plasma renin activity, or aldosterone concentration.

As shown in Fig. 1, the plasma levels of total AM, AM–NH_2, and AM–Gly were all significantly elevated in the obese subjects compared with the non-obese subjects. Table 3 shows the coefficients of correlation obtained by simple regression analyses of the relationships between two AM values and other basal, metabolic, or humoral parameters in the subjects. Both the AM–NH_2 and AM–Gly level were significantly correlated with BMI, SBP, and DBP, and significant relationships were observed between the AM–NH_2 level and age and between the AM–Gly and serum creatinine levels. In the analyses of the metabolic and humoral data, we found that the AM–NH_2 level was significantly correlated with serum triglyceride levels, while the AM–Gly level was correlated with all the parameters listed in Table 3. These significant relationships between the two AM values and BMI or metabolic or humoral factors are shown in Figs. 2 and 3 by scattered plotting.

We further analyzed the relationships by means of multivariate analysis with a step-wise method in order to identify the independently significant factors for the two AM values. As shown in Table 4, BMI and the serum triglyceride levels were found to be independently significant for the AM–NH_2 level, while DBP, insulin and HDL-cholesterol levels, and plasma renin activity were significant for the AM–Gly level. To look at gender differences in plasma AM levels, we also carried out multivariate analysis including gender in addition to the significant parameters presented in Table 3, but gender was not extracted as a significant factor of the plasma levels of AM–NH_2 or AM–Gly.

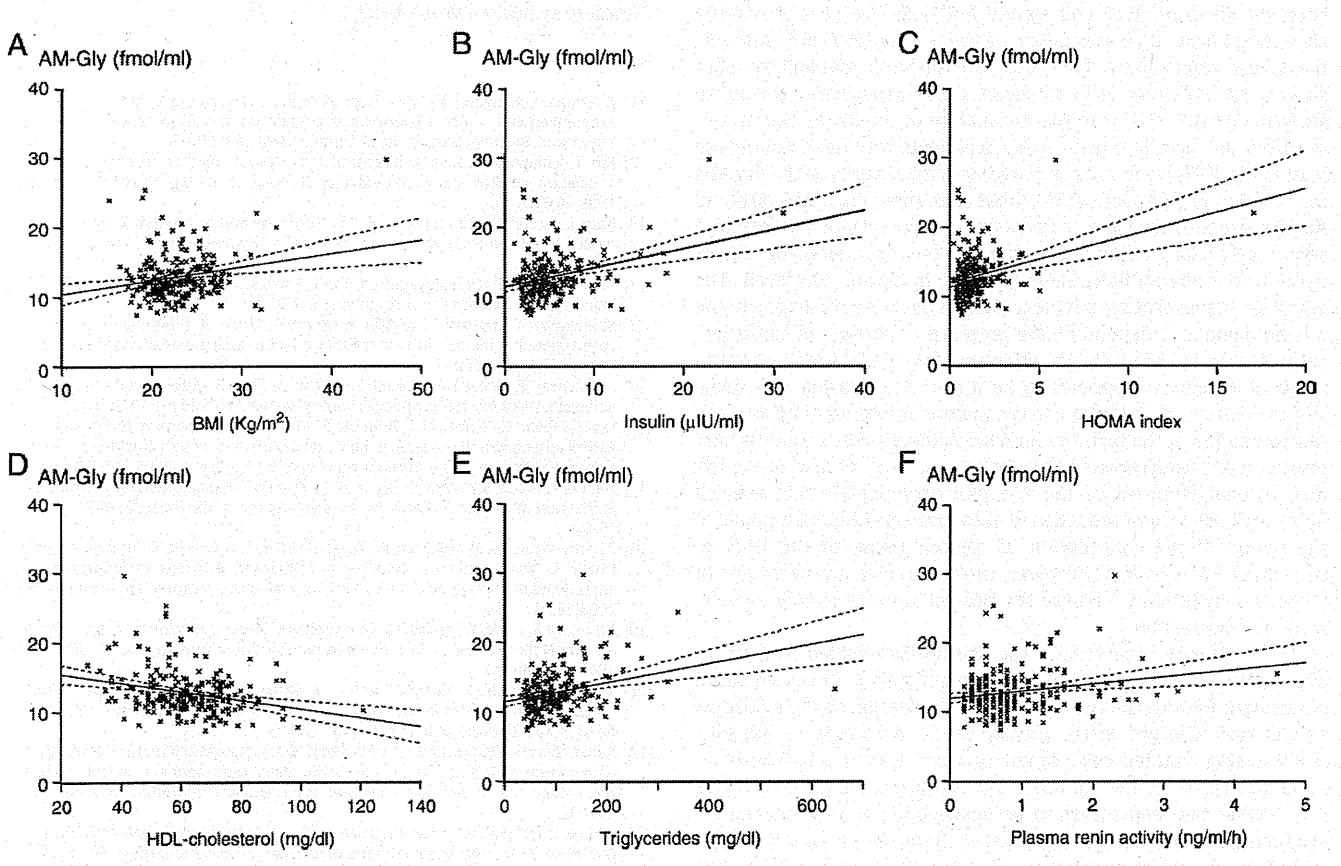

Fig. 3. Relationships between the AM–Gly and BMI (A), insulin (B), HOMA index (C), HDL-cholesterol (D), triglyceride (E) levels, or plasma renin activity (F). Regression lines and 95% confidence limits are shown on each graph.

Table 4
Multiple regression analysis with a step-wise method.

Dependent variables	Independent covariates	β	P
AM–NH_2	BMI	.185	.006
	Triglycerides	.154	.022
AM–Gly	DBP	.210	.001
	Insulin	.177	.008
	HDL-cholesterol	−.178	.006
	Plasma renin activity	.177	.005

The independent covariates included in this analysis were those judged to be significant by the simple regression analysis (Table 3).
The abbreviations are listed in Tables 1 and 2.

4. Discussion

Two molecular forms of AM circulate in the blood of humans and rats; one is a mature form of AM with an amidated C-terminal (AM–NH_2), and the other is an intermediate form with a non-amidated C-terminal glycine (AM–Gly) [14,18]. There are a number of reports on AM measurements in plasma and tissue, but in most of these cases, the immunoreactive AM detected was the total AM level consisting of both AM–NH_2 and AM–Gly [2–4,14]. Using a radioimmunoassay to detect total AM levels, we have previously reported a significant relationship between plasma AM levels and BMI in subjects who had undergone a regular medical check-up [12], and an obesity-related increase in the plasma AM level has also been reported in an animal model of obesity [8]. In the present study, we measured the plasma levels of AM with two types of immunoreactive radiometric assays that detect total and mature AM, respectively, and found that both the AM–NH_2 and AM–Gly levels were elevated in subjects with obesity according to their BMI, as compared to those who were not obese.

Cultured cells isolated from the blood vessels or myocardium have been shown to produce and secrete AM [3,4]. We have previously shown significant increases in the plasma levels of AM–NH_2 between the femoral artery and vein and between the aortic root and coronary sinus in patients with ischemic heart disease, suggesting the active secretion of AM–NH_2 from the vasculature of the lower extremities and from the heart in humans [19]. In patients with heart failure, the plasma AM–NH_2 levels are correlated with the severity of the disease, but not with BMI or obesity [20]. It has been shown that AM–NH_2 and AM–Gly are produced and secreted from adipose tissue and cultured adipocytes [7,8,21], a finding that suggests the contribution of adipose tissue to the obesity/BMI-related increase in plasma AM levels. The organs or tissues that contribute to the AM peptides circulating in the human blood may depend on the presence or absence of cardiovascular disease. For example, in patients with heart failure, the cardiac tissue or vasculature appears to be a source of plasma AM, while adipose tissue may contribute to the mature or intermediate forms of AM circulating in the blood of humans without overt cardiovascular disease. It has been reported that the plasma levels of total AM or the mid-regional fragment of the AM precursor peptide are reduced following body weight reduction in obese patients [22,23], supporting the notion of the contribution of adipose tissue to the level of circulating AM peptides. However, further studies are necessary to prove this hypothesis, because the present study is simply a cross-sectional observation.

The mechanism involved in the obesity/BMI-related increase in plasma AM levels remains to be clarified but may be discussed based on previous findings obtained by in vitro studies and on the statistical correlations observed in the present study. According to previous studies using cultured cells, tumor necrosis factor-α (TNF-α) is an important factor for the stimulation of AM production in adipocytes [21]. TNF-α has been shown to be involved in the development of insulin resistance [24,25]. In the present study, the AM–Gly level was related to metabolic parameters of insulin resistance such as the HOMA index, HDL-cholesterol, and triglycerides, suggesting a role for TNF-α in the BMI/obesity-related increase. We may also need to note the significant correlation between the AM–Gly level and plasma renin activity, because the renin–angiotensin system has been shown to be an important factor for stimulating AM production and secretion [2–4]. In the present study, the findings of interest include the differences in the correlation coefficients obtained by simple regression and in the significant factors demonstrated by the multivariate analysis between AM–NH_2 and AM–Gly. According to our previous studies [14,26,27], it is possible that the AM–NH_2 levels in plasma depend on at least two factors: enzymatic amidation activity and peptide clearance by receptor binding. These factors may have been involved in producing the different results of the simple and multiple regression analyses between AM–NH_2 and AM–Gly.

Lastly, we need to discuss the role(s) of AM–NH_2 and AM–Gly in plasma, the levels of which were elevated in relation to increased BMI and/or obesity. AM has been shown to have a wide range of actions including blood pressure reduction, modulation of adipogenesis, and alleviation of insulin resistance [2–7]. AM–Gly itself is biologically inactive, but we showed that AM–Gly exerts vasodilatory action following conversion into AM–NH_2 in isolated rat aortas ex vivo [27]. In this experiment, AM–Gly took a much longer time to reach the maximal relaxation than did AM–NH_2, suggesting a role for AM–Gly as a hormone reservoir. Based on the correlations between the two molecular forms of AM and the other clinical parameters, we speculate that AM acts against the development of a number of obesity-induced disorders such as insulin resistance and elevated blood pressure.

In conclusion, the present study showed that both the AM–NH_2 and AM–Gly levels in plasma are elevated in subjects with increased BMI or obesity without overt cardiovascular disease. The correlations between the plasma AM levels and the other clinical parameters suggest a possible, active role for this bioactive peptide in metabolic disorders associated with obesity.

References

[1] Kitamura K, Kangawa K, Kawamoto M, Ichiki Y, Nakamura S, Matsuo H, Eto T. Adrenomedullin: a novel hypotensive peptide isolated from human pheochromocytoma. Biochem Biophys Res Commun 1993;192:553–60.
[2] Eto T, Kitamura K, Kato J. Biological and clinical roles of adrenomedullin in circulation control and cardiovascular diseases. Clin Exp Pharmacol Physiol 1999;26:371–80.
[3] Kato J, Tsuruda T, Kitamura K, Eto T. Adrenomedullin: a possible autocrine or paracrine hormone in the cardiac ventricles. Hypertens Res 2003;26(Suppl): S113–9.
[4] Kato J, Tsuruda T, Kita T, Kitamura K, Eto T. Adrenomedullin: a protective factor for blood vessels. Arterioscler Thromb Vasc Biol 2005;25:2480–7.
[5] Shimosawa T, Ogihara T, Matsui H, Asano T, Ando K, Fujita T. Deficiency of adrenomedullin induces insulin resistance by increasing oxidative stress. Hypertension 2003;41:1080–5.
[6] Harmancey R, Senard JM, Rouet P, Pathak A, Smih F. Adrenomedullin inhibits adipogenesis under transcriptional control of insulin. Diabetes 2007;56:553–63.
[7] Iemura-Inaba C, Nishikimi T, Akimoto K, Yoshihara F, Minamino N, Matsuoka H. Role of adrenomedullin system in lipid metabolism and its signaling mechanism in cultured adipocytes. Am J Physiol Regul Integr Comp Physiol 2008;295:R1376–84.
[8] Nambu T, Arai H, Komatsu Y, Yasoda A, Moriyama K, Kanamoto N, Itoh H, Nakao K. Expression of the adrenomedullin gene in adipose tissue. Regul Pept 2005;132: 17–22.
[9] Paulmyer-Lacroix O, Desbriere R, Poggi M, Achard V, Alessi MC, Boudouresque F, Ouafik L, Vuaroqueaux V, Labuhn M, Dutourand A, Grino M. Expression of adrenomedullin in adipose tissue of lean and obese women. Eur J Endocrinol 2006;155:177–85.
[10] Kitamura K, Ichiki Y, Tanaka M, Kawamoto M, Emura J, Sakakibara S, Kangawa K, Matsuo H, Eto T. Immunoreactive adrenomedullin in human plasma. FEBS Lett 1994;341:288–90.
[11] Kato J, Kobayashi K, Etoh T, Tanaka M, Kitamura K, Imamura T, Koiwaya Y, Kangawa K, Eto T. Plasma adrenomedullin concentration in patients with heart failure. J Clin Endocrinol Metab 1996;81:180–3.
[12] Kato J, Kitamura K, Uemura T, Kuwasako K, Kita T, Kangawa K, Eto T. Plasma levels of adrenomedullin and atrial and brain natriuretic peptides in the general population: their relations to age and pulse pressure. Hypertens Res 2002;25: 887–92.
[13] Ishimitsu T, Nishikimi T, Saito Y, Kitamura K, Eto T, Kangawa K, Matsuo H, Omae T, Matsuoka H. Plasma levels of adrenomedullin, a newly identified hypotensive peptide, in patients with hypertension and renal failure. J Clin Invest 1994;94: 2158–61.

[14] Kitamura K, Kato J, Kawamoto M, Tanaka M, Chino N, Kangawa K, Eto T. The intermediate form of glycine-extended adrenomedullin is the major circulating molecular form in human plasma. Biochem Biophys Res Commun 1998;244: 551–5.
[15] Examination Committee of Criteria for 'Obesity Disease' in Japan. Japan Society for the Study of Obesity: new criteria for 'obesity disease' in Japan. Circ J 2002;66: 987–92.
[16] Ohta H, Tsuji T, Asai S, Sasakura K, Teraoka H, Kitamura K, Kangawa K. One-step direct assay for mature-type adrenomedullin with monoclonal antibodies. Clin Chem 1999;45:244–51.
[17] Ohta H, Tsuji T, Asai S, Tanizaki S, Sasakura K, Teraoka H, Kitamura K, Kangawa K. A simple immunoradiometric assay for measuring the entire molecules of adrenomedullin in human plasma. Clin Chim Acta 1999;287:131–43.
[18] Yamaga J, Hashida S, Kitamura K, Tokashiki M, Aoki T, Inatsu H, Ishikawa N, Kangawa K, Morishita K, Eto T. Direct measurement of glycine-extended adrenomedullin in plasma and tissue using an ultrasensitive immune complex transfer enzyme immunoassay in rats. Hypertens Res 2003;26(Suppl):S45–53.
[19] Hirayama N, Kitamura K, Imamura T, Kato J, Koiwaya Y, Eto T. Secretion and clearance of the mature form of adrenomedullin in humans. Life Sci 1999;64: 2505–9.
[20] Hirayama N, Kitamura K, Imamura T, Kato J, Koiwaya Y, Tsuji T, Kangawa K, Eto T. Molecular forms of circulating adrenomedullin in patients with congestive heart failure. J Endocrinol 1999;160:297–303.
[21] Li Y, Totsune K, Takeda K, Furuyama K, Shibahara S, Takahashi K. Differential expression of adrenomedullin and resistin in 3T3-L1 adipocytes treated with tumor necrosis factor-alpha. Eur J Endocrinol 2003;149:231–8.
[22] Minami J, Nishikimi T, Ishimitsu T, Makino Y, Kawano Y, Takishita S, Kangawa K, Matsuoka H. Effect of a hypocaloric diet on adrenomedullin and natriuretic peptides in obese patients with essential hypertension. J Cardiovasc Pharmacol 2000;36(Suppl 2):S83–6.
[23] Vila G, Riedl M, Maier C, Struck J, Morgenthaler NG, Handisurya A, Prager G, Ludvik B, Clodi M, Luger A. Plasma MR-proADM correlates to BMI and decreases in relation to leptin after gastric bypass surgery. Obesity 2009;17:1184–8.
[24] Hotamisligil GS, Peraldi P, Budavari A, Ellis R, White MF, Spiegelman BM. IRS-1-mediated inhibition of insulin receptor tyrosine kinase activity in TNF-alpha- and obesity-induced insulin resistance. Science 1996;271:665–8.
[25] Uysal KT, Wiesbrock SM, Marino MW, Hotamisligil GS. Protection from obesity-induced insulin resistance in mice lacking TNF-alpha function. Nature 1997;389: 610–4.
[26] Ishiyama Y, Kitamura K, Ichiki Y, Sakata J, Kida O, Kangawa K, Eto T. Haemodynamic responses to rat adrenomedullin in anaesthetized spontaneously hypertensive rats. Clin Exp Pharmacol Physiol 1995;22:614–8.
[27] Cao YN, Kitamura K, Ito K, Kato J, Hashida S, Morishita K, Eto T. Glycine-extended adrenomedullin exerts vasodilator effect through amidation in the rat aorta. Regul Pept 2003;113:109–14.

Cephalalgia
An International Journal of Headache
International Headache Society

doi:10.1111/j.1468-2982.2008.01695.x

Effect of adrenomedullin on the cerebral circulation: relevance to primary headache disorders

KA Petersen[1,2], S Birk[1,2], K Kitamura[3] & J Olesen[1,2]

[1]Danish Headache Centre, University of Copenhagen, Copenhagen and [2]Department of Neurology, Glostrup University Hospital, Glostrup, Denmark, and [3]First Department of Internal Medicine, Miyazaki Medical College, University of Miyazaki, Miyazaki, Japan

Cephalalgia

Petersen KA, Birk S, Kitamura K & Olesen J. Effect of adrenomedullin on the cerebral circulation: relevance to primary headache disorders. Cephalalgia 2009; 29:23–30. London. ISSN 0333-1024

Adrenomedullin (ADM) is closely related to calcitonin gene-related peptide, which has a known causative role in migraine. Animal studies have strongly suggested that ADM has a vasodilatory effect within the cerebral circulation. For these reasons, ADM is also likely to be involved in migraine. However, the hypothetical migraine-inducing property and effect on human cerebral circulation of ADM have not previously been investigated. Human ADM (0.08 μg kg^{-1} min^{-1}) or placebo (saline 0.9%) was administered as a 20-min intravenous infusion to 12 patients suffering from migraine without aura in a crossover double-blind study. The occurrence of headache and associated symptoms were registered regularly 24 h post infusion. Cerebral blood flow (CBF) was measured by ^{133}Xenon single-photon emission computed tomography, mean blood flow velocity in the middle cerebral artery (V_{MCA}) by transcranial Doppler and the diameter of peripheral arteries by transdermal ultrasound (C-scan). ADM did not induce significantly more headache or migraine compared with placebo ($P = 0.58$). CBF was unaffected by ADM infusion (global CBF, $P = 0.32$ and $rCBF_{MCA}$, $P = 0.38$) and the same applied for the V_{MCA} ($P = 0.18$). The superficial temporal artery dilated compared with placebo ($P < 0.001$), and facial flushing was seen after ADM administration ($P = 0.001$). In conclusion, intravenous ADM is not a mediator of migraine headache and does not dilate intracranial arteries. □*Adrenomedullin, cerebral blood flow, vasodilatation, migraine*

Kenneth A. Petersen, MD, PhD, Danish Headache Centre, University Hospital of Copenhagen and Department of Neurology, Glostrup University Hospital, DK-2600 Glostrup, Denmark. Tel. +45 3810-0448, e-mail kapetersen@dadlnet.dk *Received 16 August 2007, accepted 1 May 2008*

Introduction

There is strong evidence of a pivotal role of calcitonin gene-related peptide (CGRP) and nitric oxide (NO) in migraine pathogenesis (1–6). However, other substances may be involved, and a member of the CGRP family, adrenomedullin (ADM), is an obvious candidate for further investigation.

ADM was discovered 10 years ago among peptides extracted from pheochromocytomas (7). Subsequently, its pharmacological and physiological properties have been defined (8). The mRNA of the peptide, originating from a single locus on chromosome 11 (9), is found in the highest concentration in endothelial cells (10) and in particular within the cerebral circulation (11). From the precursor molecule two circulating products are formed, the inactive intermediate form (ADM_{gly}) and the active mature form (ADM). Being a secreted product of the vascular endothelium along with NO and endothelin, ADM is largely distributed according to tissue vascularity.

ADM activates a combined calcitonin receptor-like receptor (CRLR) and the receptor activity modifying protein (RAMP2), possibly RAMP3, coupled receptor and increases the formation of intracellular

cAMP (12). The best-described effect of ADM is vasodilation, but the exact function in human physiology and pathophysiology, including up-regulation during inflammation, remains to be determined. In healthy volunteers, administered ADM dose-dependently decreases systolic and diastolic blood pressure (BP) and increases heart rate (HR) (13, 14). Facial flushing, conjunctival injection and mild headache have furthermore been described. Headache was observed in six of eight subjects and, respectively, in one out of 11 subjects (15, 16) after ADM administration.

ADM receptors are situated on the endothelial and smooth muscle cells of cerebral vessels and ADM is produced within cerebral endothelial cells, in contrast to CGRP, which is released from perivascular sensory nerve endings. CGRP does not seem to play an important role in the maintenance of resting tone of cerebral vessels (17), whereas ADM might do so at high plasma levels (11).

The properties of ADM and its similarity to CGRP, as well as the possible activation of CGRP receptors by ADM, make it an obvious candidate to be involved in migraine mechanisms. We therefore conducted this double-blind study to evaluate whether ADM affects the cerebral and extracranial haemodynamics and whether it causes headache or migraine in migraine suffers.

Methods and patients

Design and patients

A placebo-controlled, double-blind, crossover design was applied in the study. The number of patients ($n = 12$) to be included was estimated according to Pocock (18) and based on the following assumptions: the probability of inducing a migraine attack on active days was set at 0.5 and on placebo days to 0.1, α to 5% and β to 10%. Fourteen patients were included, but two were excluded due to development of claustrophobia during the baseline single-photon emission computed tomography (SPECT) scan. In all, 12 patients completed both treatment days.

The migraine patients all fulfilled the criteria of the International Headache Society (IHS) (19) for migraine without aura (MoA) and had a maximum of six attacks per month. A second diagnose of tension-type headache was allowed with a maximum of four episodes per month. Entry criteria were: MoA (19) and age 18–65 years. Exclusion criteria were: present or previous cardiovascular, cerebrovascular, endocrine or neurological disorder, prophylactic treatment for migraine and concomitant medication that might influence the outcome measures.

The study population consisted of 10 women and two men with a mean age of 41 years (range 28–50 years). Written informed consent was obtained before randomization. The Ethical Committee of Copenhagen (KA01115s) and the Danish Medicines Agency (2612-1771) approved the study, which was conducted according to the Helsinki II declaration. A balanced randomization was performed using Medstat©. A double-blind, crossover design was used. Placebo (0.9% NaCl) or human ADM ($0.08\ \mu g\ kg^{-1}\ min^{-1}$) was administered intravenously in a balanced randomized order on the two different trials days. h-ADM(1-52) was purchased from Clinalfa AG (Bubendorf, Switzerland) and diluted in 0.9% isotonic saline immediately before administration.

The choice of ADM dose was partly based on previously published studies using doses between 0.016 and $0.081\ \mu g\ kg^{-1}\ min^{-1}$ and partly on a dose finding pilot study including three patients suffering from MoA. In a single trial day they received three intravenous (i.v.) cumulative doses of ADM [0.06, 0.08 and $0.1\ \mu g\ kg^{-1}\ min^{-1}$ (i.v.)] as 20-min infusions separated by a 60-min wash-out period. The first patient developed severe tachycardia, increasing BP, peripheral vasoconstriction and cold sweating after the 0.1-μg dose. Therefore, the two remaining patients received only 0.06 and $0.08\ \mu g\ kg^{-1}\ min^{-1}$ of ADM (i.v.), which was well tolerated.

Headache and adverse events

Every 10 min from baseline to T_{120} (end of study period) the patients were questioned for the presence of headache, associated symptoms and adverse events (AEs). Between questionings the patients self-reported any changes they might experience. The intensity of the AEs was graded as mild, moderate or severe and their relationship to ADM was classified as related or not related by the investigator. Headache intensity was scored on an 11-point verbal rating scale with 0 = no headache, 1 = mild headache or a sensation of pressing or throbbing inside the head, not necessarily felt as actual pain, 5 = medium severe headache, 10 = worst imaginable headache. Accompanying symptoms were recorded according to the IHS (19). After discharge, patients made an hourly recording of headache up to 24 h after the infusion of placebo or ADM.

Cerebral blood flow measurements

Global and regional cerebral blood flow (CBF) was measured with ^{133}Xenon inhalation and SPECT with a brain-dedicated camera (Ceraspect; DSI, Waltham, MA, USA). The apparatus consists of a stationary annular NaI crystal and a fast rotating collimator system. Each rotation took 10 s, thereby acquiring one frame in a 30-frame dynamic protocol of ^{133}Xenon inhalation, three background, nine wash-in, 18 wash-out using the Kanno-Lassen algorithm (20). A photoelectric window of 70–100 keV was employed.

Thirty-two slices were reconstructed in a 64×64 matrix with each pixel measuring 0.33×0.33 cm using a Butterworth 1D filter (cut-off 1.5, order 6). The 32 slices were reduced to sets of eight transaxial slices generated by adding four slices together to a total slice thickness of 1.32 cm. Attenuation correction using the Chang algorithm ($\mu = 0.05$ cm) and correction for nose artefact was performed. The output for each pixel was the k_i-value and flow values were estimated from these using the partition coefficient (λ) of 0.85 ml/g (grey matter).

A Datex Normocap 200 (Dameca, Roedovre, Denmark) was used for end-tidal CO_2 measurements during the CBF acquisitions. A Ceratronic XAS SM 320 (Randers, Denmark) was used for the ^{133}Xenon administration. Each measurement lasted 5 min.

Calculations of flow in the perfusion territories of the major cerebral arteries were performed fitting standard vascular regions of interest on the five slices at 3.6, 5.0, 6.3, 7.6 and 9 cm above the orbitomeatal line. Flow in the territory of the middle cerebral artery (MCA) ($rCBF_{MCA}$) was calculated as a mean of the left and right side.

Transcranial Doppler and C-scan

Transcranial Doppler (TCD) ultrasonography (2 MHz, Multidop X Doppler; DWL, Sipplingen, Germany) was used for the measurement of blood flow velocity. The recordings were done simultaneously and bilaterally as previously described, but with handheld probes (21). Along the MCA, a fixed point was found for the measurement. The fixed point was chosen as close as possible to the bifurcation of the anterior cerebral artery and MCA. The same fix-point was used for each individual and for each recording, at which the signal was optimized. Based upon the envelope curve (spectral TCD curve), a time-average mean (V_{mean}) over approximately four cardiac cycles (4 s) was calculated by the built-in software (TCD software for MDX 7.40x). The final measure used for each time point was an average of four cycles (V_{MCA}). Simultaneously with the TCD recording, a mask covering the subjects' mouth and nose region was placed for the measurement of end-tidal pCO_2 ($P_{et}CO_2$) (Datex Normocap 200; Dameca).

A high-resolution ultrasound scanner, C-scan (Dermascan C, 20 MHz, bandwidth 15 MHz; Hadsund, Denmark) was used to measure the diameter of the left temporal and left radial arteries (22). The diameter of the former was measured at the front branch of the superficial temporal artery (STA) and the latter at the wrist. To ensure that the repeated measurements with TCD and C-scan were performed in the same place, marks were drawn on the skin. After the last recording on the first trial day, the coordinates of the marks were recorded for re-use on the following trial day.

Pharmacokinetics

At the beginning of each trial day the haematocrit value was determined. Plasma samples for the analysis of ADM concentration (ADM_{Total} and ADM_{Mature}) were obtained four times during each trial day (T_{-20}, $T_{19.5}$, T_{60} and T_{120}). The plasma samples were collected in cooled 10-ml K3 ethylenediamine tetraaceticacid vacutainers containing Apropotinin (Trasylol© 0.6 antecubital unit/ml blood) from the cubital vein contralateral to the site of ADM or placebo infusion. The samples were immediately placed on ice and subsequently centrifuged for 10 min (1500 *g*) at 4°C. Plasma was stored at –30°C until analysed at the University of Miyazaki, Japan. The applied assay for measurement of ADM has previously been validated (23, 24).

Trial procedures

The migraine patients began the study at 07.45 h with a short interview ensuring the following inclusion criteria: no migraine attack or tension-type headache for the preceding 48 h, no intake of triptans or analgesics, e.g. paracetamol, within the same period of time, no intake of ergotamine for the previous 72 h and abstinence from coffee, tea, caffeine-containing drinks and smoking tobacco for the preceding 8 h. The patients rested supine throughout the study period.

Two i.v. catheters [Optiva*2, (18G); Johnson & Johnson, Ethicon S.p.A., Italy] were inserted into the cubital veins, one for the administration of

placebo or h-ADM, the other for blood sampling. The volunteers rested at least 30 min before baseline values of CBF, V_{MCA}, temporal and radial diameter, BP, HR and electrocardiogram (ECG) were recorded. The start of infusion of h-ADM or placebo was designated time zero (T_0). The infusion lasted 20 min and was administered by a time- and volume-controlled infusion pump (Braun® perfusor; B. Braun, Melsungen, Germany).

The SPECT measurements were repeated twice at T_{25} and T_{115}. Every 10 min from T_{-20} until T_{120} questioning for headache and associated symptoms followed by measurement of TCD and C-scans were performed. BP, HR (Omega 1400; In vivo Research Laboratories Inc., Copiague, NY, USA) and ECG (Cardiofax; Nihon Kohden Corp., Tokyo, Japan) were recorded at T_{-20}, T_{-10}, T_0 and thereafter every 5 min throughout the study.

$rCBF_x$ in the area of a given artery (x) is related to mean blood flow velocity ($V_{mean(x)}$) and cross-sectional area, $\pi \times r^2$, of the artery.

$$rCBF_{(x)} = V_{mean(x)} \times \pi \times r^2$$

If the rCBF changes the following equation is valid:

$$\Delta Diameter = \left(\left(\sqrt{\frac{rCBF_{2(x)}/Vmean_{2(x)}}{\times\, Vmean_{1(x)}/rCBF_{1(x)}}}\right) - 1\right) \times 100$$

Δ Diameter is the relative percent change in diameter; $V_{mean1(x)}$ is the mean blood velocity before infusion of drugs and $V_{mean2(X)}$ the velocity at a relevant time point after the infusion. The same nomination is applied for rCBF (25, 26).

Statistics

Baseline was calculated as a mean of the values at T_{-20}, T_{-10} and T_0. Values are presented as means ± S.D. $P < 0.05$ was considered significant. All analyses were performed using SPSS statistical software version 10.0 (SPSS Inc., Chicago, IL, USA).

For changes over time on each trial day global CBF, $rCBF_{MCA}$, V_{MCA}, diameter of the temporal and radial artery, BP, HR and $P_{et}CO_2$ were analysed by univariate analysis of variance for the factors time and subject. If a significant change was found, a *post hoc* analysis (Dunnett's multiple comparisons test) was performed to localize the change. To eliminate the risk of mass significance on measurements with numerous repeated measurements, four points of interest were chosen: baseline, 20 min, 60 min and 120 min. Absolute values were used for the statistical analysis. For the comparison between ADM and placebo a paired *t*-test was performed for the following measurements: global CBF, $rCBF_{MCA}$, V_{MCA}, diameter of the temporal and radial artery, BP, HR and $P_{et}CO_2$. Summary measure for the *t*-test was the area under the curve (AUC) calculated on percentage changes from baseline.

Immediate headache was defined as any headache during the first 60 min after the start of the h-ADM administration. Any headache occurring thereafter was called delayed headache. Peak values and $AUC_{Headache}$ (area under the headache curve) were compared between the two trial days using Wilcoxon's signed rank test. The occurrence of headache and AEs on the two trial days was compared with McNemar's test.

Results

Baseline characteristics

No significant differences were found between the two experimental days in values of haemodynamic variables, haematocrit or start and end room temperature.

Headache and associated symptoms

Of the 12 included patients, six experienced immediate headache on days with administration of ADM and one on placebo days ($P = 0.13$). Four patients had a delayed headache on placebo days and seven after ADM ($P = 0.38$). Figure 1 shows the headache score of the individual patients. Analysis of the peak headache revealed no difference between ADM and placebo for the immediate ($P = 0.17$) or delayed ($P = 0.87$) period. Based on the $AUC_{Headache}$, a tendency towards difference in the immediate period was found ($P = 0.051$), but none was detected for the entire registration ($P = 0.58$) or delayed period ($P = 0.78$). The experienced headache fulfilled the IHS criteria for MoA in six cases. Two patients had MoA on both trial days, and in the remaining four patients two after ADM and two after placebo administration.

ADM induced flushing in all patients and placebo in one ($P = 0.001$), 11 patients experienced heat sensation after ADM and four after placebo ($P = 0.016$).

Pharmacokinetics

Baseline plasma concentration of ADM_{total} (11.67 ± 2.43 fmol/ml and 11.09 ± 2.7 fmol/ml) and ADM_{mature} (2.78 ± 0.68 fmol/ml and 2.77 ± 0.58 fmol/ml) were similar on the two trial days.

The C_{max} of ADM_{total} (76.4 ± 16.6 fmol/ml) and ADM_{mature} (24.4 ± 6.0 fmol/ml) were measured at time point $T_{19.5}$, at the end of the h-ADM infusion. After 2 h the plasma levels had not yet returned to baseline (Fig. 2). On placebo days no change from the baseline values were recorded.

Cerebral and peripheral haemodynamics

There were no significant differences in baseline values between ADM and placebo administration days (Table 1). After ADM there was no change in global CBF ($P = 0.32$ $P_{et}CO_2$ uncorrected, and $P = 0.22$ $P_{et}CO_2$ corrected) or in $rCBF_{MCA}$ ($P = 0.38$, $P_{et}CO_2$ uncorrected, and $P = 0.27$ $P_{et}CO_2$ corrected) compared with placebo (Fig. 3). Global CBF and $rCBF_{MCA}$ increased significantly ($P = 0.034$ and $P = 0.035$) over time after ADM when the measurements were corrected for $P_{et}CO_2$. The increase was only seen 5 min after termination of the infusion. However, without $P_{et}CO_2$ correction no significant increase was seen ($P = 0.097$ and $P = 0.096$). On placebo days no change over time was seen. $P_{et}CO_2$ measured during CBF acquisition did not change over time, and there was no difference between treatments ($P = 0.32$).

$P_{et}CO_2$-corrected V_{MCA} increased significantly over time after ADM ($P = 0.027$). The difference from baseline was recorded at time point T_{20} and was 6.6 ± 2.4%. For the left MCA alone ($V_{MCA(left)}$) a similar result was obtained ($P = 0.023$). The right

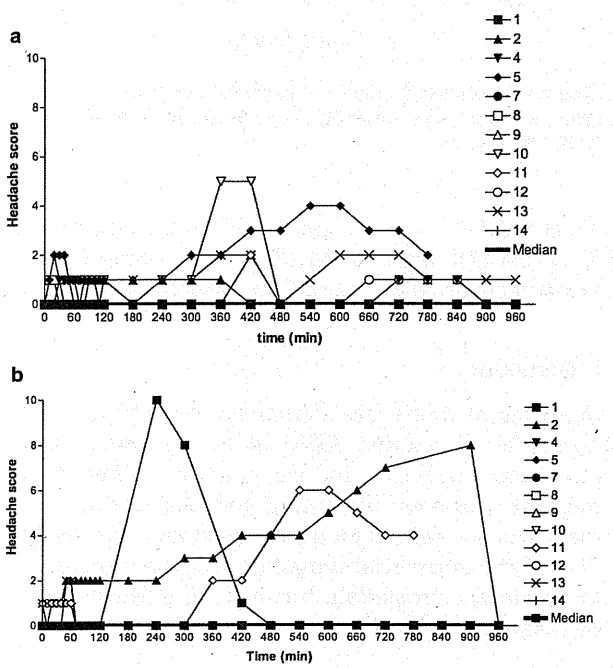

Figure 1 Individual curves of headache scores for all patients on days of h-ADM infusion (a) and placebo (b). The median headache score is in bold.

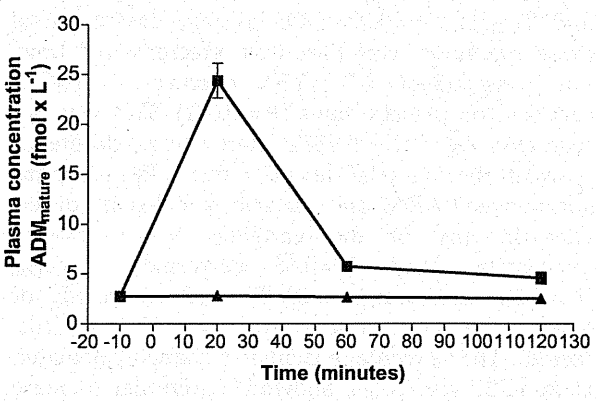

Figure 2 Plasma concentration of ADM_{Mature} on the two trial days; ■, h-ADM; ▼, placebo.

Table 1 Baseline values on the two trial days with comparison using a paired *t*-test

	Adrenomedullin		Placebo		
	Mean	(±) S.D.	Mean	(±) S.D.	*P*
$V_{MCA\ left}$ (cm/s)	74.74	13.15	78.92	13.32	0.085
$V_{MCA\ right}$ (cm/s)	77.66	11.84	81.49	13.81	0.171
$V_{MCA\ mean}$ (cm/s)	76.20	11.36	80.20	12.86	0.081
pCO_2 (mmHg)	36.75	4.29	37.75	4.61	0.255
Radial artery (mm)	2.35	0.52	2.36	0.56	0.965
Temporal artery (mm)	1.11	0.28	1.09	0.19	0.791
Systolic BP (mmHg)	116.94	11.82	116.17	13.62	0.724
Diastolic BP (mmHg)	72.42	8.00	73.08	8.95	0.780
Mean BP (mmHg)	86.90	8.40	88.03	10.62	0.618
Heart rate (bpm)	61.01	9.45	61.75	7.84	0.639

BP, blood pressure.

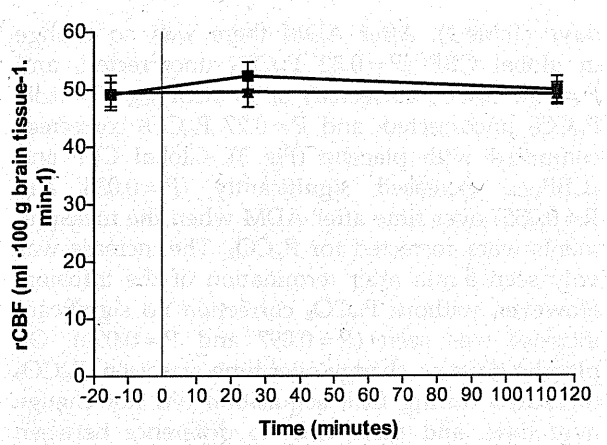

Figure 3 rCBF (ml 100 g brain tissue^{-1} min^{-1}) vs. time (minutes) for, respectively: ■, h-ADM administered; ▼, placebo. Vertical line = initiation of infusion.

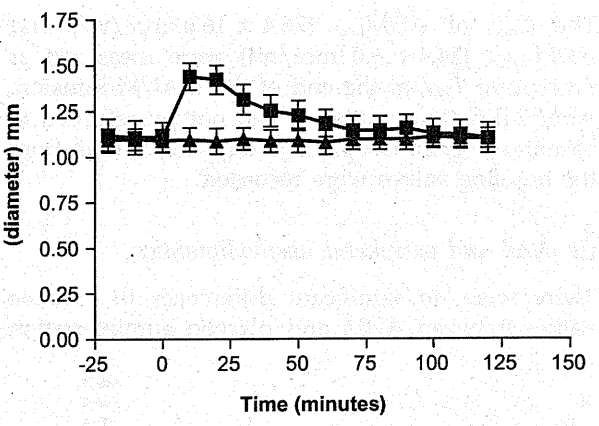

Figure 4 Diameter change in superficial temporal (mm) artery vs. time (minutes) for, respectively: ■, h-ADM AND; ▼, placebo.

MCA ($V_{MCA(right)}$) was not significantly affected by the ADM. Without $P_{et}CO_2$ correction, none of the significant increases was observed, V_{MCA} ($P = 0.069$) and $V_{MCA(left)}$ ($P = 0.078$). On placebo days none of these measured variables was affected over time, but a significant 6.3 ± 1.5% decrease in $P_{et}CO_2$ occurred on placebo days ($P = 0.001$). This was not seen after ADM ($P = 0.155$). There was no difference between the two trial days ($P = 0.30$). The comparison between ADM and placebo revealed no difference in any of the variables V_{MCA} ($P = 0.18$ uncorrected and $P = 0.66$ corrected), $V_{MCA(left)}$ ($P = 0.36$ uncorrected and $P = 0.97$ corrected) or $V_{MCA(right)}$ ($P = 0.12$ uncorrected and $P = 0.42$ corrected). The percentage diameter change calculated from rCBF and V_{MCA} showed a minimal increase (1.2% ± 3.5%) at T_{25} after ADM, and there was no difference between trial days ($P = 0.72$).

Temporal artery diameter increased significantly compared with placebo ($P = 0.01$), whereas the radial artery diameter was unchanged after ADM compared with placebo ($P = 0.38$). ADM increased the temporal artery diameter over time ($P < 0.001$), the maximal increase being recorded at T_{10} and 33.42 ± 6.22%. The temporal ($P = 0.47$) and radial artery diameter ($P = 0.53$) was unaffected over time after placebo, as was the radial diameter after ADM ($P = 0.21$) (Fig. 4).

There were no significant changes after ADM compared with placebo in systolic BP ($P = 0.23$), diastolic BP ($P = 0.9$) or mean BP ($P = 0.86$). HR was significantly increased after ADM ($P = 0.003$) compared with placebo. ADM induced a significant decrease in systolic BP ($P = 0.03$), diastolic BP ($P < 0.001$, −9.53 ± 1.93%) and mean BP ($P < 0.001$, −7.63 ± 2.41%) over time. HR was increased 33.77 ± 4.17% after ADM ($P < 0.001$). None of the measured variables changed on placebo days.

Discussion

The present study has demonstrated that intravenously administrated ADM at the maximal tolerated dose did not induce migraine attacks in migraine patients, indicating that ADM does not play a major role in migraine pathogenesis. ADM dilated the superficial temporal artery and affected the systemic circulation, but had no effect on CBF or diameter of MCA.

Haemodynamic effects of ADM

Meeran and co-workers administered ADM to healthy volunteers and found that a low dose of ADM (3.2 pmol kg^{-1} min^{-1}) did not affect BP or HR, whereas a higher dose (13.4 pmol kg^{-1} min^{-1}) resulted in a significant decrease in diastolic BP (69 ± 2 to 53 ± 2 mmHg) and a significant increase in HR (57 ± 3 to 95 ± 4 bpm) (13). With a dose of 0.05 μg kg^{-1} min^{-1} Nagaya et al. found smaller effects, but a significantly increased cardiac index and decreased pulmonary arterial pressure in patients with chronic heart failure (15). Long-term administration of AM in lower doses (2.9 and 5.8 pmol kg^{-1} min^{-1}) showed a minor effect on systemic haemodynamics (14, 16). Administering 0.08 μg kg^{-1} min^{-1} for 20 min, we found that the systolic, diastolic and mean arterial BP were unaffected by ADM compared with placebo. HR was significantly increased.